Altered fatty acid metabolism rewires cholangiocarcinoma stemness features

Giulia Lori, Mirella Pastore, Nadia Navari, Benedetta Piombanti, Richell Booijink, Elisabetta Rovida, Ignazia Tusa, Monika Lewinska, Jesper B. Andersen, Tiziano Lottini, Annarosa Arcangeli, Maria Letizia Taddei, Erica Pranzini, Caterina Mancini, Cecilia Anceschi, Stefania Madiai, Elena Sacco, Stefano Rota, Adriana Trapani, Gennaro Agrimi, Matteo Ramazzotti, Paola Ostano, Caterina Peraldo Neia, Matteo Parri, Fabrizia Carli, Silvia Sabatini, Amalia Gastaldelli, Fabio Marra, Chiara Raggi

Table of contents

Supplementary materials and methods

Cell culture and reagents

CCLP1, HUCCT1 and SG231 cells, from intrahepatic bile duct cancer tissue, were kind gift from Dr. AJ Demetris, University of Pittsburgh. iCCA4 were provided by Prof Domenico Alvaro Sapienza University of Rome, Italy. Cell lines were cultured as described (1,2). BSA, oleic acid, palmitoleic acid, fluorescein 5(6)-isothiocyanate (FITC) were purchased from Sigma Aldrich. Orlistat was purchased from MedChem Express. Dialysis tubes with a MWCO 1200-14000 Da were purchased from Spectra Labs (Rome, Italy).

Sphere formation assay

The cells were grown in anchoring-independent conditions into poly 2-hydroxyethyl methacrylate (poly-HEMA)-coated dishes (Sigma Aldrich) with selective serum-free DMEM/F12 medium supplemented with 1X B27 supplement without vitamin A (Life Technologies), 20 ng/mL EGF, and 20 ng/mL bFGF (R&D Systems) (1, 2). To determine SPH-forming ability, 500 CCA cells/well in a 96 multiwell were grown in anchoring-independent conditions with selective serum-free medium. After 7 days, pictures were taken to measure the number and size of CCA-SPH using a Leica DMi1microscope (Leica). Average number of formed spheres microscopic field (20x) over five fields. CCA-SPH volume was calculated after measuring length 1 (L1) and the length 2 (L2) using the following formula: V = (L1*L2*L2)/2.

Quantitative real-time polymerase chain reaction (RT-PCR)

Total RNA was extracted with the RNeasy kit (Qiagen) according to the manufacturer's instructions. The RNA concentration and quality were determine using an optical NanoDrop ND1000 spectrophotometer (ThermoFisher Scientific). Total RNA (1 µg) was retro transcribed with a High-Capacity cDNA Reverse Transcription Kit (Applied Biosystems). Relative gene expression was calculated using $2^{-\Delta\Delta Ct}$ method. The mRNA levels of Actin were used for normalization. Results shown are the mean of three different experiments ± SD. Sequences of used primers are listed in Supplemental Table 6.

Western blot analysis

Cells were lysed at 4°C with lysis buffer (1% Triton X-100, 50 mmol/L Tris–HCl, pH 7.4, 150 mmol/L NaCl, 1 mmol/L EDTA, 1 mmol/L sodium orthovanadate, 2 mmol/L PMSF, and 1 mmol/L each of leupeptin and pepstatin). After 30 minutes of lysis, cellular extracts were centrifuged for 20 min at 14000 rpm, and the supernatant was used for Western blot experiments as detailed elsewhere (2). Antibodies were used according to the manufacturer's

instructions. Immunoblot were incubated overnight at 4°C with primary antibody in 1% BSA in PBS. Primary antibodies are listed in Supplemental Table7.

Then, immunoblot were incubated with secondary antibody α-rabbit/mouse (1:4000) in 1% BSA in 1x DPBS for 1hour, then with Horseradish peroxidase (HRP)-conjugated tertiary antibody α-rabbit/mouse Monoclonal anti-β-actin antibodies produced in mouse (A5441, Sigma) or monoclonal anti-vinculin antibodies produced in mouse (V9131, Sigma) were used as internal control (1:1000). Quantification of the signal was obtained by chemiluminescence detection on an Image Quant Las4000 (GE Healthcare Life Sciences) and subsequent analysis conducted with ImageJ software.

Cell survival assay

A total of $8x10^4$ CCA cells were seeded in 96 multiwell plate and serum starved for 24h. Then cells were treated with oleic or palmitoleic acid for 24 hours and with cisplatin or oxaliplatin for further 24 hours. Medium was removed and a 0.5% crystal violet solution in 20% methanol was added. After 5 min of staining, the fixed cells were washed with phosphate-buffered saline (PBS) and solubilized with 100 µl/well of 0.1 M sodium citrate, pH 4.2. The absorbance at 595 nm was evaluated using a microplate reader (HiPo biosan, Bio Class).

Annexin V/PI staining

A total of $1x10^5$ CCA cells were seeded in 6 multiwell dishes and serum starved for 24h. Then cells were treated with oleic or palmitoleic acid for 24h and with cisplatin or oxalilplatin for further 24hours. Cells were detached, counted and stained with Annexin V-FLUOS Staining Kit according to the manufacturer's instructions. The percentage of both early and late apoptotic cells were detected and measured using FACSCanto II (BD Biosciences).

Cell cycle analysis

In total, 80 000 cells/well were seeded in 6 multiwell dishes and exposed to the appropriate conditions. After medium removal, 400 µl of solution containing 50 µg/mL propidium iodide, 0.1% w/v trisodium citrate and 0.1% NP40 was added. Samples were then incubated for 30 min at 4°C in the dark and nuclei analyzed with an FACSCanto II (BD Biosciences).

Cell proliferation assay

A total of $10x10^4$ cells were plated in 96 multiwell plate and incubated in medium deprived of serum for 24 hours. Cells were exposed to different stimuli and then proliferation was evaluated by BrdU incorporation using the Cell Proliferation ELISA-BrdU (colorimetric) Kit (Roche) according to the manufacturer's protocols. SPH were dissociated and seeded in a 96-well plate and allowed to grow overnight in SPH medium with 1% FBS.

Aldehyde Dehydrogenase (ALDH) activity detection

ALDH activity was measured in iCCA spheres with different treatments using Aldehyde Dehydrogenase Activity Colorimetric Assay kit (Merck) following manufacturer's instruction.

Migration assay

Migration was measured in Boyden chamber equipped with 8 μm pore filters (Millipore Corp) coated with rat tail collagen (20 μg/ml) (Collaborative Biomedical Products, Bedford, UK), as described in detail elsewhere (2). After six hours incubation at 37 °C, cells migrated to the underside of the filters were fixed, stained with Diff Quick, mounted and counted at 40X magnification. The values for migration were expressed as the average number of migrating cells per microscopic field over five fields. Each experiment was performed in triplicate.

Cell transfection

Control siRNA and siFASN were purchased from Dharmacon. Cells were transfected as previously described (2) using the Amaxa nucleofection technology (Amaxa) according to manufacturer's instructions. CCLP1 cells were transfected with FASN human shRNA plasmid (#TR313058, Origene) or scrambled shRNA (#TR30012, Origene) using Lipofectamine 3000 (Thermofisher) according to the protocol. Transfected cells were established by selection with Puromycin.

FAO assay kit

Fatty acid beta oxidation was measured with FAO assay kit (Assay Genie) following the manufacturer's protocols.

BODIPY staining

MON and SPH cells were stained with 2 μm BODIPY 493/503 (Cayman Chemicals) in the dark at 37°C for 15 mins. Cells were harvested by trypsinization, washed twice and analyzed by flow cytometry with FACSCanto II (BD Biosciences). For confocal microscopy, cells were incubated with 2 μm BODIPY and 5 μm Hoechst for 15 mins in the dark at 37°C. Then, cells were washed twice in PBS and fixed in 4% PFA for 15 minutes at room temperature. PFA was removed and viewed by a confocal microscope (TCS SP8; Leica).

Lipidomic analysis

For lipidomic analysis three replicates of each cell line (CCLP1 MON n=3, CCLP1 SPH n=3, HUCCT1 MON n=3, HUCCT1 SPH n=3) were cultured for 48 hours with a medium enriched with 10% deuterated water. About one million of cells were homogenized with 300 of methanol

µl (or the volume was adjusted according to the number of cells) and 20ul of the mix of internal standards were added to the sample. Samples were put on oscillating plate for 30 minutes at 4°C and centrifuged at 14000 rpm. After centrifugation, the methanol surnatant was transferred to the vials for injection and analysis. Lipid classes were separated with UHPLC 1290 Infinity (Agilent) equipped with ZORBAX Eclipse Plus C18 2.1x100mm 1.8 µm column (Agilent), and untarget acquisition of all lipids was performed by LC/MS-QTOF (Agilent UHPLC 1290 Infinity-6540 QTOF) in positive ion ionization. The concentrations of a selected panel of lipids previously found relevant for liver disease (3) were quantified with internal standard, i.e., TG (15:/15:0/15:0) (Larodan), Ceramide (d18:1/17:0), Sphingomyelin (d18:1/17:0), Lysophosphatidylcholine (17:0), Phosphatidylcholine (17:0/17:0), Phosphatidylethanolamine (17:0/17:0), Lysophosphatidylethanolamine (17:1) (Avanti Polar Lipids, Alabaster, AL). For heatmap representation, lipids concentration levels were scaled to zero mean and unit variance and reported as median within the four groups. *De novo* TAGs synthesis was evaluated by measurement the deuterium incorporation using isotopologue extraction in Agilent MassHunter Profinder B.08.00 software. *De novo* TAGs synthesis was reported as % of labeled TGs in the total amount of single species. Desaturation was evaluated as ratio between monounsaturated to saturated TAGs.

Gene expression

Total RNA (3 µg) from in vivo mouse tumors was reverse transcribed using QuantiNova Reverse Transcription kit (Qiagen). RT-PCR was performed using QuantiNova LNA PCR Focus Panel Human Liver Cancer 384-well plates (SBHS-133ZE, Qiagen). In each 384-well plate, a number of 4 different tumor samples for each group were tested for 84 genes specifically associated with liver cancer pathways. The expression values were calculated with the ΔΔCt method, using the average of ACTB, GAPDH, RPLP0 and HPRT1 as housekeeping genes as reference. A cutoff of at least 1.5-fold increases and 0.5-fold decreases were considered significant.

In addition, same tumor samples for each group were tested for 31 genes associated with stemness features (CSC, EMT and drug transporters; TableS2). Total RNA (1 µg) from in vivo mouse tumors was retro transcribed with a High-Capacity cDNA Reverse Transcription Kit (Applied Biosystems). Relative gene expression was calculated using $2^{-\Delta\Delta Ct}$ method. The mRNA levels of Actin were used for normalization. Data are mean ± SEM (n=3). A cutoff of at least 1.5-fold increases and 0.5-fold decreases were considered significant.

Immunochemistry staining

From the *in vivo* experiment, tumor samples for each group were tested for -PCNA expression. The histological analysis of tumor mass was performed as described below. Removed tumors

were fixed at 4°C in 10% neutral buffered formalin (BioOptica, Milan) for histological analysis performed on paraffin-embedded sections (5 μm). Immunohistochemistry was performed using the Leica BOND-MAX™ automated system (Leica Microsystems). The expression of mouse monoclonal anti-PCNA (#2586, 1:8000, Cell Signaling Technology) was evaluated. Slides were developed with 3′3-diaminobenzidine DAB (Leica Microsystems) and counterstained with hematoxylin. For antibodies used on mouse tissues, the blocking Mouse on Mouse (M.O.M.) basic kit (Leica Microsystem) was used according to the manufacturer's datasheet. All sections were examined using an optical microscope and photos were acquired using Leica Scanner Aperio CS2 (Leica).

Microarray Data Analysis

Correlation of FASN expression with survival was performed by stratifying 68 iCCA patients (4) by median expression of FASN and generation of Kaplan-Meier curves. Survival curves were compared with the log-rank test (Prism 9.4.1). Spearman correlation of FASN expression with SOX2, NOTCH1, VEGFA, and ABCG2 was performed using log2 transformed expression signals (Prism 9.4.1). The univariate association of FASN expression with clinical pathological was performed with Fisher's exact test for categorical parameters and t-test for continuous data in iCCA patients stratified by median FASN expression.

Ultrasound and photoacoustic in vivo imaging

Tumor volumes were determined in vivo imaging system (Vevo LAZR-X photoacoustic imaging). High-resolution ultrasound (US) imaging was done performing 3D acquisition in B-Mode on live mice, by using VevoLAZR-X imaging station (Fujifilm Visualsonics). The acquisitions to evaluate the tumor growth were performed weakly, starting from the day before the first treatment, until the experimental endpoint. During the analysis, mice were anesthetized with a continuous flow of isoflurane (initial induction at 4% and maintenance at 2%) and placed on a mouse handling table, heated at 37°C, in prone position. ECG, respiration rate and body temperature were monitored during the analysis. 55-MHz transducer was used for echography. Data obtained were analyzed using Vevo LAB software (Fujifilm Visualsonics) to measure the tumor volumes.

Library preparation and RNA-sequencing

Total RNA was isolated from cells using the miRNeasy Mini Kit (Qiagen) according to the manufacturer's protocol. Total-RNA-sequencing (RNA-seq) library preparation was performed starting from 100 ng of total-RNA with the SMARTer Stranded Total RNA Sample Prep Kit - Low Input Mammalian (Clontech-Takara). The libraries obtained were qualitatively and qualitatively assessed by using TapeStation 4200 (Agilent) and quantified by Qubit

Fluorimeter (ThermoFisher). Afterwards, they were multiplexed in an equimolar pool and sequenced on a NextSeq-500 Illumina Platform generating more than 60 million 75bp Paired End reads (bp-PE) per sample.

Reads preprocessing

Sequencing data was demultiplexed into separate, adapter free compressed fastq files using bcl2fastq v2.20.0.422 (Illumina, Inc.) and a reference sample sheet specifying for each sample the corresponding barcode. Reads were further processed using the fastp program (5) configured to use 20 threads for removing read pairs with at least 50% of bases with Q > 30, a minimal length of 70 bp, a complexity > 30%. No trimming was performed on reads.

Reads alignment, abundance estimation and differential analysis

Reads mapping was performed using the default options but specifying the --numGibbsSamples 500 and -validateMappings options, on a reference transcriptome composed by the union of the human cDNA and ncDNA available from Ensembl (assembly GRCh38.p13) indexed with a kmer size of 23 by Salmon v0.14.1 (6). Reads were imported into R using the tximport package (7) with the “Salmon” specific method. Gene level abundance was estimated from transcript level estimates using the summarizeToGene function of tximport working on a transcript to gene association table (further associating gene names for functional analysis, see below) obtained with Ensembl Biomart system (8) operating on Ensembl genes 98/GRCh38.p13 human genes. Data matrices were eventually converted in DEseq2 objects using the DESeqDataSetFromTximport function, specifying the SPH vs MON phenotypes as the design contrast.

Functional analysis

For the functional analysis of the experiment the GSEA 4.0.2 software by BROAD Institute was used (9,10) in the GSEAPreRanked mode using the Wald-statistic from the DESeq2 analysis as input metric for sorting. Gene lists were obtained from MSigDB 7.0 (11,12) and gene names were converted into Ensembl gene IDs using a simple perl script reading the same table produced by Biomart used for gene abundance estimation (see above). A selection of interesting gene sets from the different MSigDB collections (kegg, biocarta, gobp, hallmark, reactome) was obtained by a custom bash script that isolated those containing mitochondrial genes (GO:0005739:mitochondrion).

Enrichr enrichment analysis

Differentially expressed genes (DEGs) in sphere (SPH) compared to monolayer (MON) in common between the CCLP1 and HUCCT1 cells with a fold change > 2 (n=307) were used to

perform molecular function and pathway analysis by Enrichr enrichment analysis at https://maayanlab.cloud/Enrichr. The following libraries were used for the analysis: Kyoto Encyclopedia of Genes and Genomes (KEGG) pathway, MSigDB Hallmark 2020, the enrichment of transcription factors (TF) Perturbations. The p-values were calculated using Fisher exact test and corrected for multiple testing by Benjamini–Hochberg adjustment and pathways with an adjusted p-value < 0.05 were considered significant. The combined score of the pathway analysis (Table S4) is calculated using the Fisher exact test and the Z-score to sort the pathways.

Supplementary figures

Suppl.Fig.1

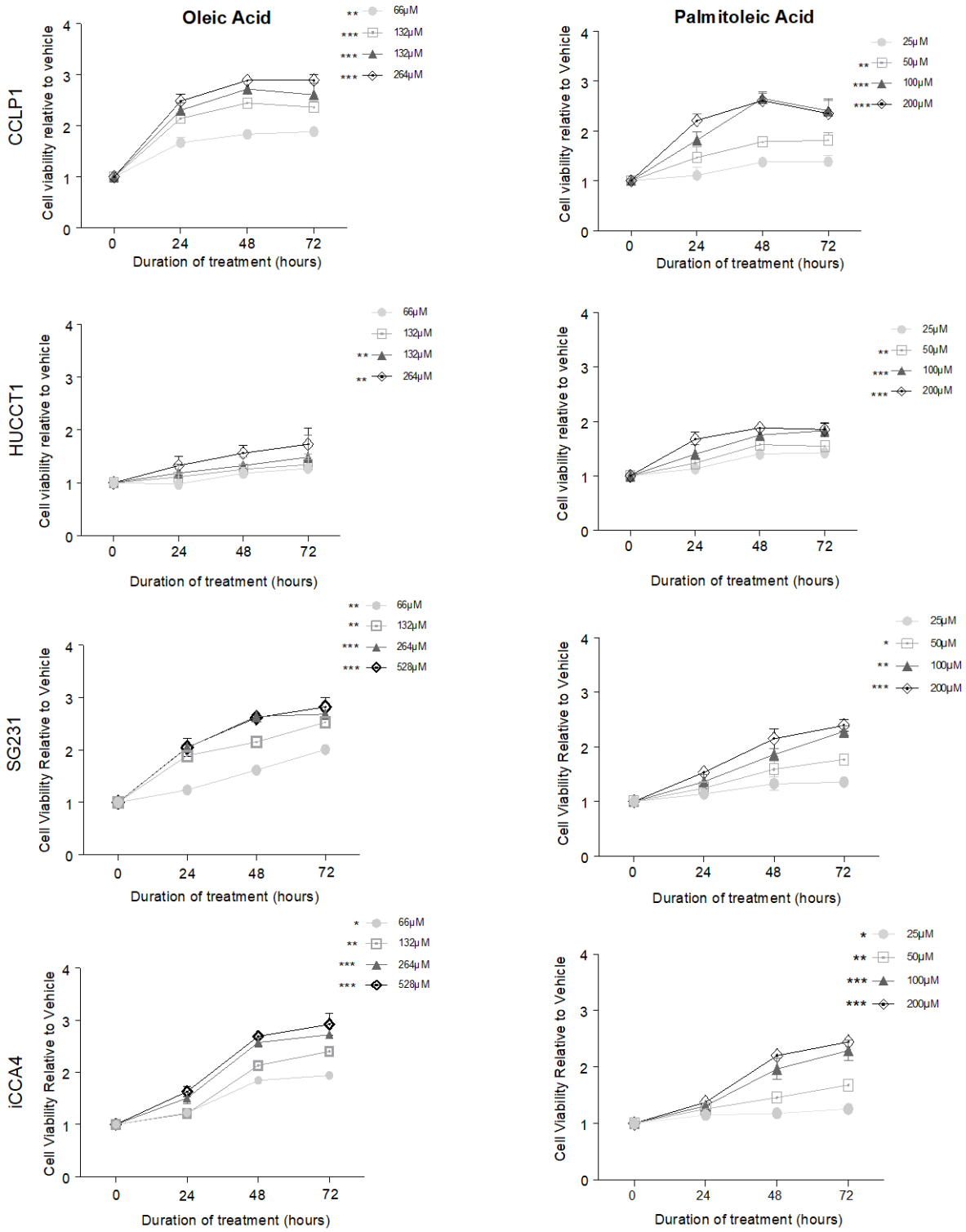

Fig. S1. Effects of oleic and palmitoleic acid on iCCA cells proliferation. Intrahepatic CCA cells were serum starved and treated with oleic or palmitoleic acid at the indicated concentration for 24, 48 and 72h in 4 iCCA cell lines (CCLP1, HUCCT1, SG231, iCCA). Then crystal violet test was performed. Results were normalized to vehicle: BSA for oleic acid and ethanol for linoleic, palmitic and palmitoleic respectively. Data are mean ± SEM (n=3, *p≤0,05, ** p≤0,01, *** p≤0,001; Mann-Whitney U test). Complete statistical data are shown in Supplementary Table 1.

Suppl.Fig.2

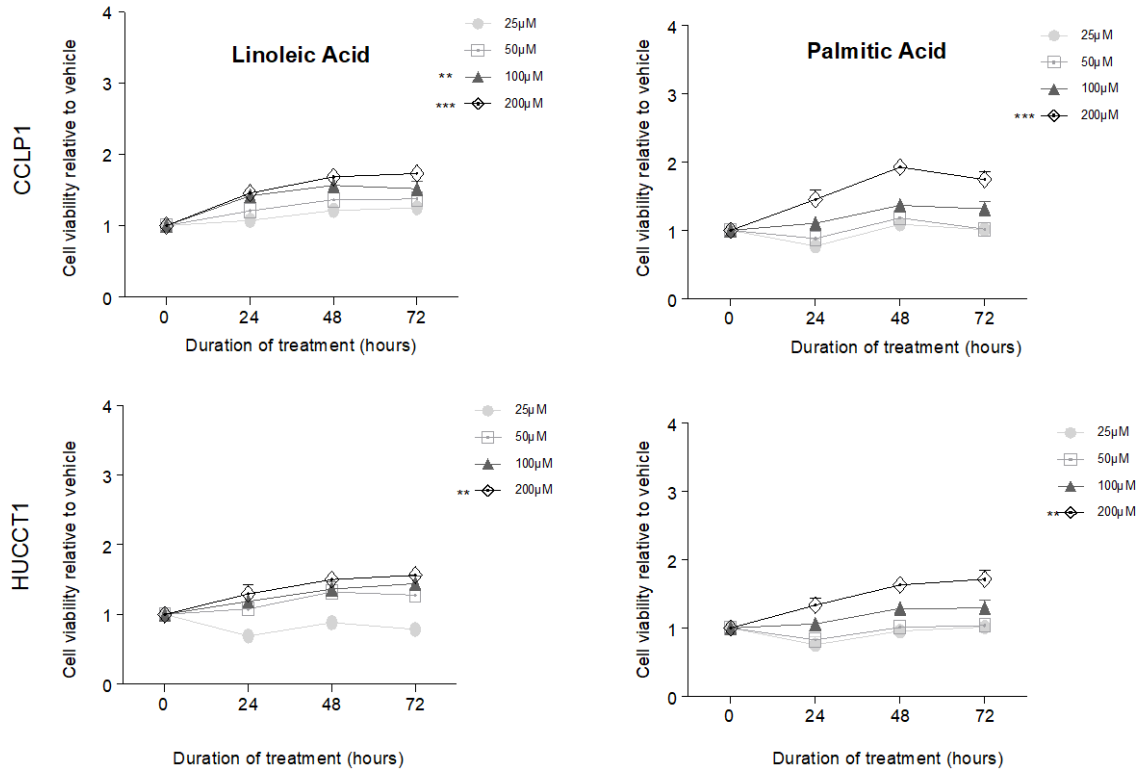

Fig. S2. Effects of linoleic and palmitic acid on iCCA cells proliferation. Intrahepatic CCA cells (CCLP1 and HUCCT1) were serum starved and treated with linoleic, palmitic, acid at the indicated concentration for 24, 48 and 72h. Then crystal violet test was performed. Results were normalized to vehicle: BSA for oleic acid and ethanol for linoleic, palmitic and palmitoleic respectively. Data are mean ± SEM (n=3, *p≤0,05, ** p≤0,01, *** p≤0,001; Mann-Whitney U test). Complete statistical data are shown in Supplementary Table 2.

Suppl.Fig.3

A

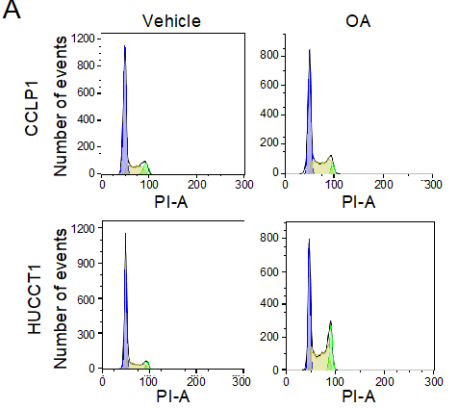

	CCLP1		HUCCT1	
	Vehicle	OA	Vehicle	OA
G0/G1	70.3 ± 9.6	59.0 ± 11.3	68.7 ± 1.1	44.6 ± 8.1**
S	19.9 ± 8.1	38.8 ± 13.0*	24.1 ± 1.3	40.2 ± 2.8***
G2/M	9.7 ± 7.9	2.2 ± 2.2*	7.2 ± 2.2	15.1 ± 5.3

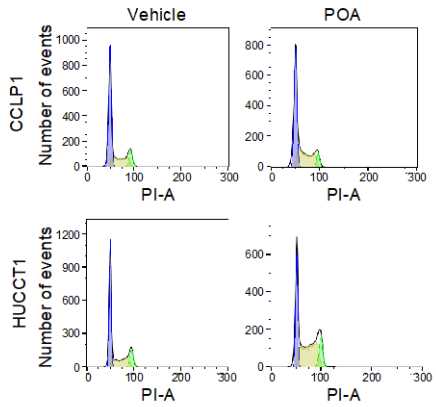

	CCLP1		HUCCT1	
	Vehicle	POA	Vehicle	POA
G0/G1	72.4 ± 11.6	49.0 ± 7.2**	53.3 ± 13.9	47.8 ± 9.7*
S	20.1 ± 12.4	42.0 ± 7.1**	28.7 ± 11.5	35.8 ± 11.9*
G2/M	7.5 ± 1.4	9.0 ± 3.3	14.2 ± 4.9	16.5 ± 6.7

B

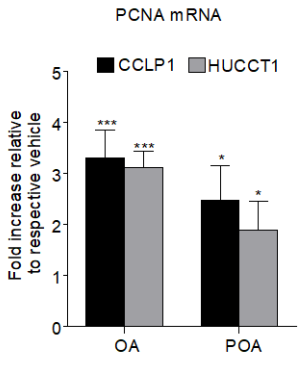

C

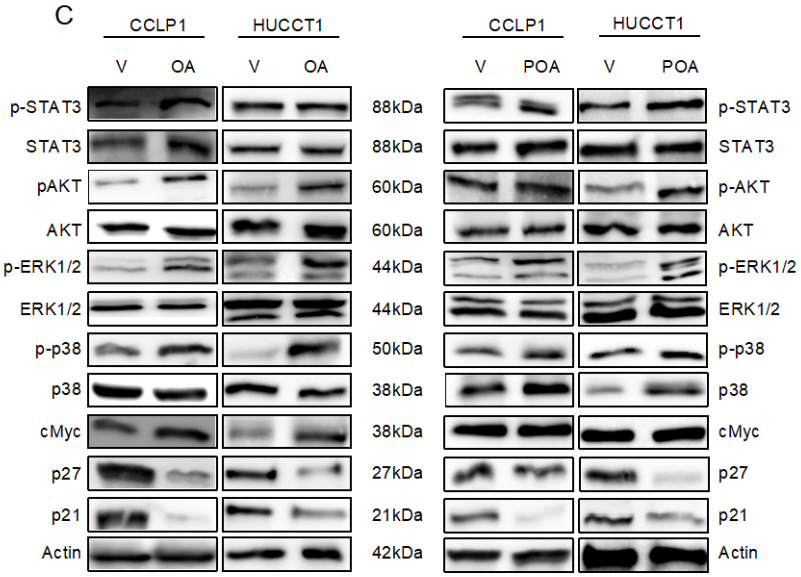

Fig. S3. Effects of monounsaturated fatty acids on cell cycle. (A) Intrahepatic CCA cells were treated in starvation medium for 48 hours with OA or POA. Cell cycle phase distribution was determined by flow cytometry. Data are mean ± SEM (n=4, *p≤0.05, **p≤0.01, *** p≤0,001; Mann-Whitney U test). (B) Intrahepatic CCA cells were treated with oleic or palmitoleic acid for 48h, then RNA was extracted. Expression of proliferating cell nuclear antigen (PCNA) gene is reported as fold changes normalized to mean expression of respective vehicle. Data are mean ± SEM (n=4, *p≤0,05, *** p≤0,001; Mann-Whitney U test). (C) Immunoblot of several proteins involved in proliferation and survival, after 48 hours MUFAs treatment in starvation medium. β-Actin immunoblot was performed to ensure equal loading.

Suppl.Fig.4

A

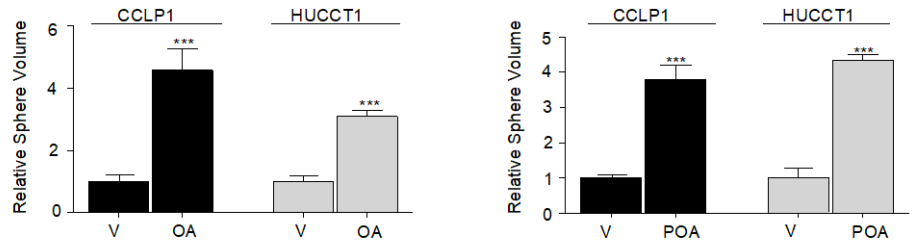

B

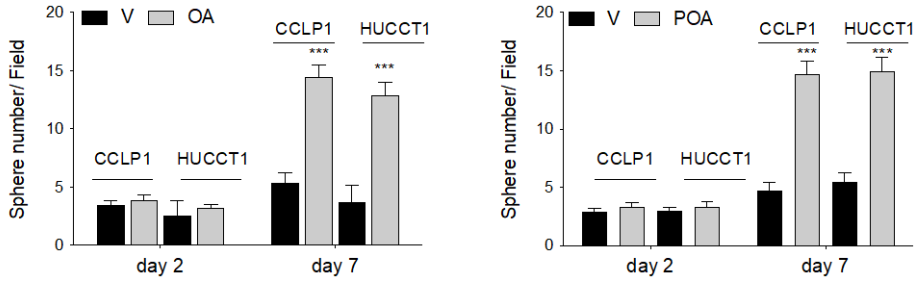

C

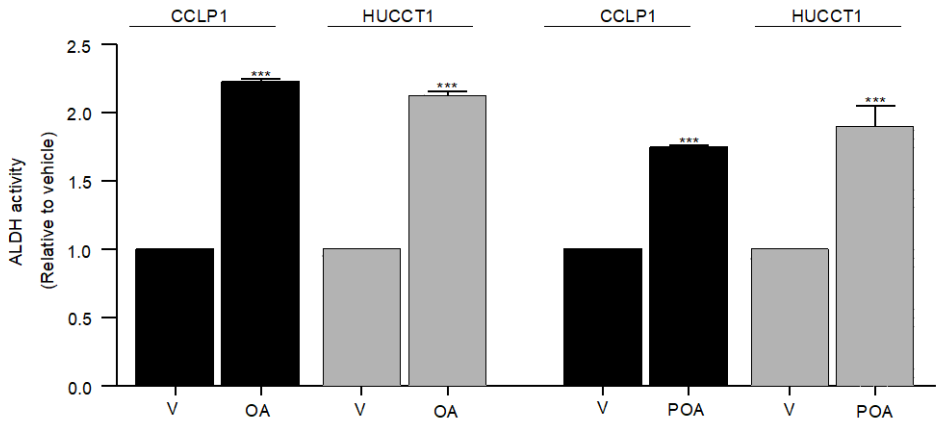

Fig. S4. Effect of MUFA on iCCA-stem-like properties. A) CCLP1 and HUCCT1 were grown as sphere (SPH) for seven days, then treated with OA or POA for 48 hours (during sphere formation). Cells have been synchronized in serum free condition, as required for cell cycle analysis. The impact of MUFAs treatment is reported as SPH volume relative to respective vehicle. Data are mean ± SEM (n=3, *** p≤0.001; Mann-Whitney U test). B) Intrahepatic CCA cells were grown were seeded in anchoring-independent conditions and treated with FAs for 48h. Then cells were grown as SPH for seven days. SPH were counted at days 2 (treatment starting) and at days 7 (end of experiment). Mean ± SEM (n=3, ***p≤0.001; Mann-Whitney U test). C) ALDH activity was determined in iCCA cells grown as SPH and treated with oleic or palmitoleic acid for 48h. Results were normalized to vehicle: BSA for oleic and ethanol for palmitoleic acid. Data are mean ± SEM (n=3, *** p≤0,001; Mann-Whitney U test).

Suppl.Fig.5

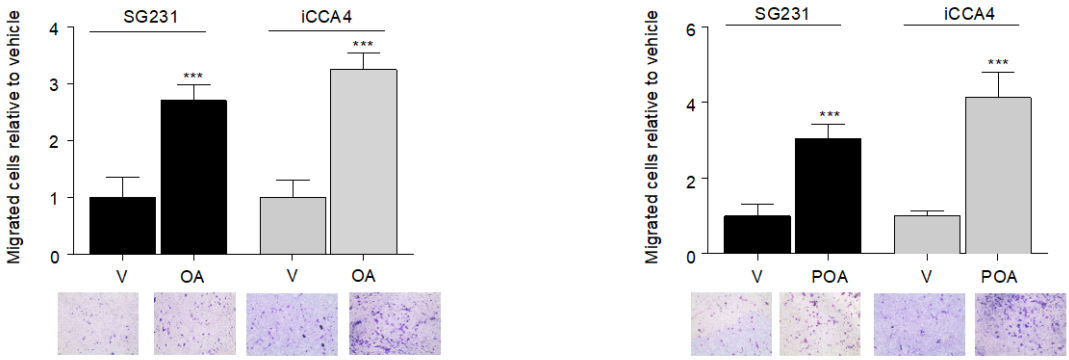

Fig. S5. Effects of oleic and palmitoleic acid on iCCA cell migration.

Migration of iCCA cells (SG231 and iCCA4) was measured in modified Boyden chambers, after 48 hours treatment. Mean ± SEM (n=3, ***p≤0.001); Mann-Whitney U test). Representative images of filters are shown below the barograms (original magnification 40x, scale bar 10µm).

Suppl.Fig.6

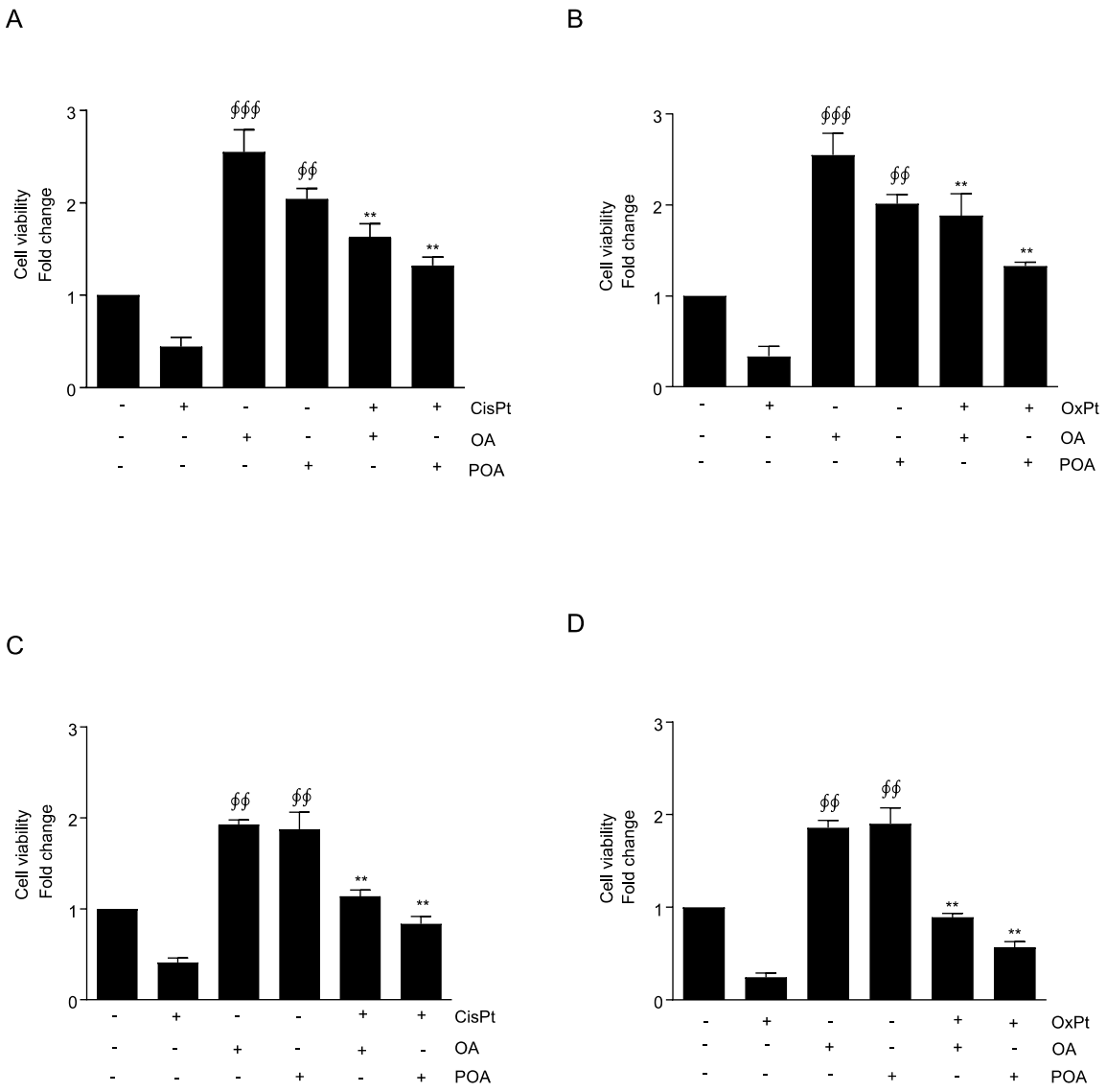

Fig. S6. **Monounsaturated FAs pretreatment protects iCCA cells from antiblastic toxic effects**. (A, B) CCLP1 and HUCCT1 cells were pretreated for 24 hours with oleic acid (OA) or palmitoleic acid (POA) in starvation medium, then with cisplatin or oxaliplatin for further 24 hours. Cell viability was assessed with crystal violet staining. Data are mean ± SEM (n=3, **p≤0.01, ***p≤0.001, ϕϕ p≤0.01, ϕϕϕ p≤0.001; Mann-Whitney U test). The * are calculated respect to cisplatin or oxalilplatin, ϕ are calculated respect to vehicle.

Suppl.Fig.7

A

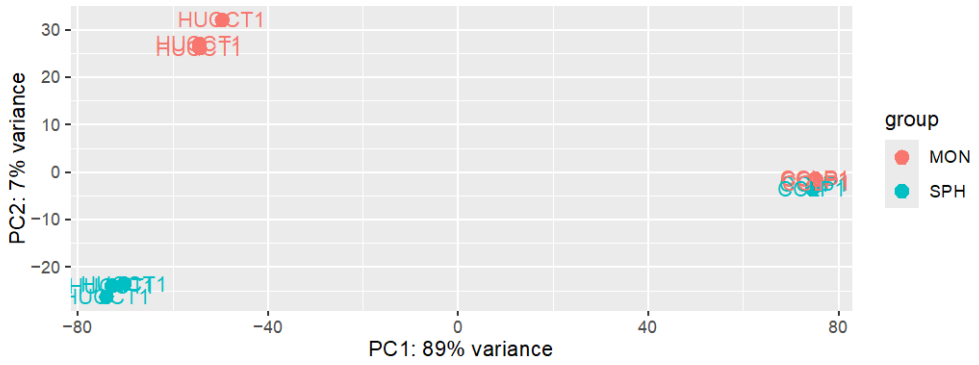

B

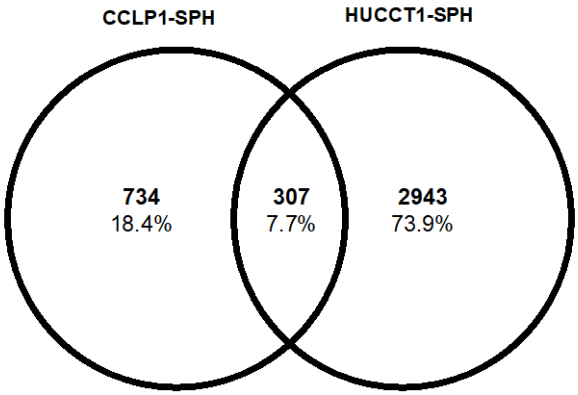

Fig. S7. Global molecular differences between sphere and monolayer cells by RNAseq analysis. A) Principal component analysis (PCA) of RNA sequeincig data of monlayer (MON) and sphere (SPH) in both CCLP1 and HUCTT1 cells. B) Venn diagram shows a total of 734 and 2943 differentially expressed genes (DEGs) in SPH compared to MON in CCLP1 and HUCCT1 respectively. Venn diagram software identified a total of 307 common DEGs in SPH.

Suppl.Fig.8

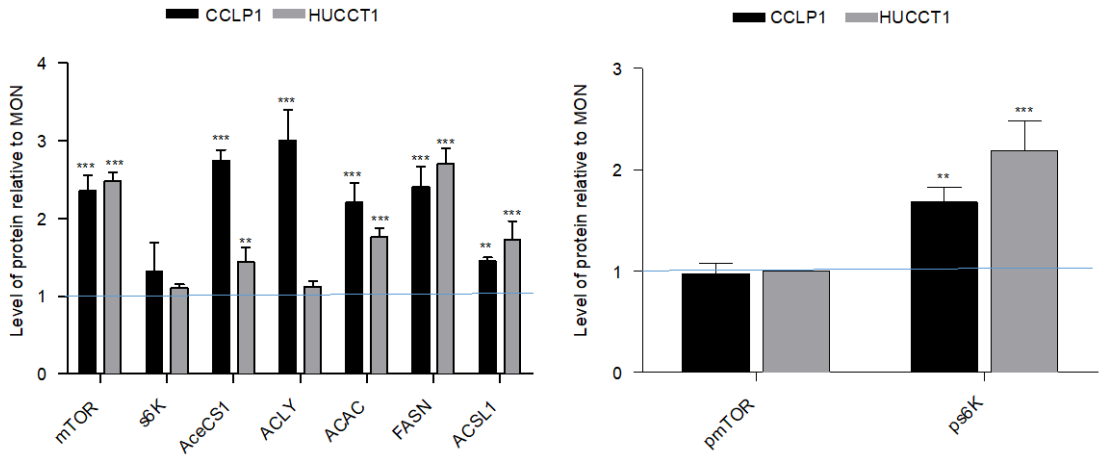

Fig. S8. Densitometric quantification of FA related proteins. Immunoblot quantification of mTOR, phospho mTOR, S6K, phosphoS6K, AceCS1, ACLY, ACAC, FASN, ACSL1 protein levels in CCLP1 and HUCCT1 cells grown as MON and SPH. mTOR, S6K, AceCS1, ACLY, ACAC, FASN and ACSL1 were normalized on β-Actin level, phospho mTOR and phosphoS6K were normalized on mTOR and S6K level, respectively. Data are shown as relative protein level respective to MON. Data are mean ± SEM (n=3, **p≤0.01, ***p≤0.001; Mann-Whitney U test).

Suppl.Fig.9

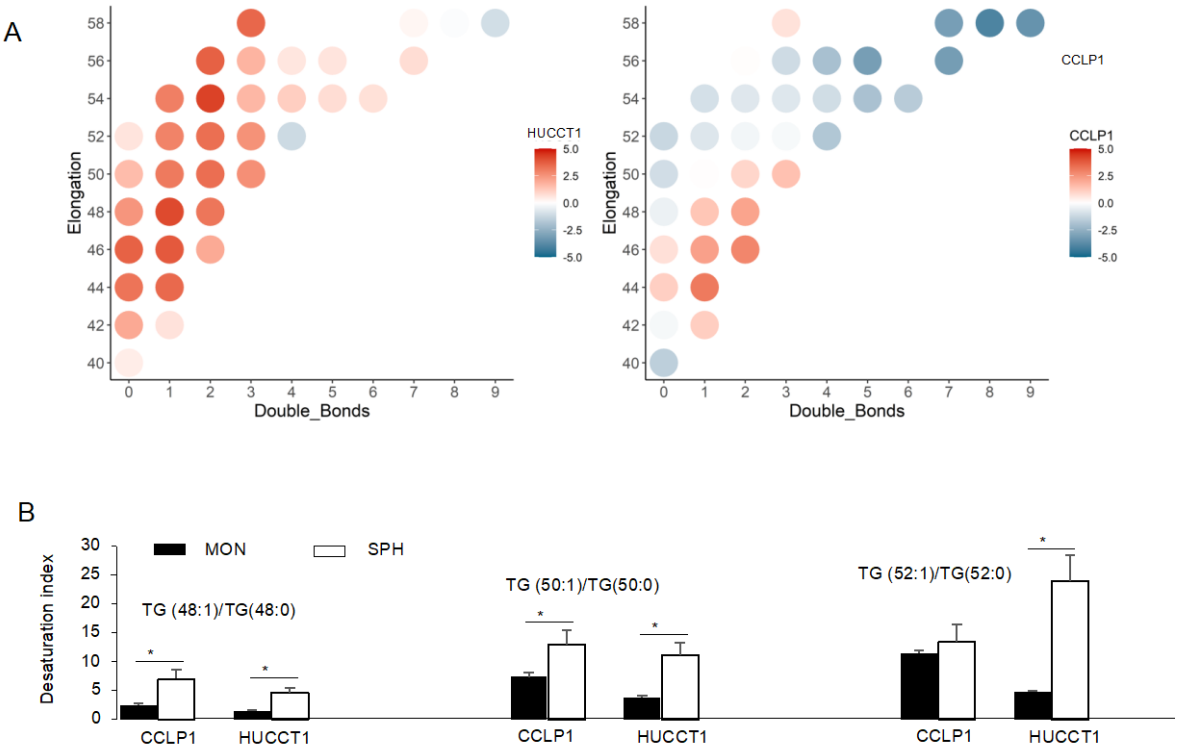

Fig. S9. Triglycerides elongation and desaturation in iCCA cells. (A) Fold change of elongation and number of double bonds of triglycerides in CCLP1 (SPH/MON) and HUCCT1 (SPH/MON). (B) Desaturation index in CCLP1 vs HUCCT1 calculated as the ratio between monounsaturated to saturated TG. Results are mean ± SEM (n=3, *p≤0,05; Mann-Whitney U test).

Suppl.Fig.10

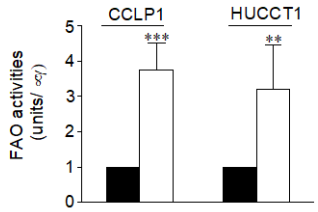

Fig. S10. Fatty acid oxidation in iCCA cells. CCLP1 and HUCCT1 cells were cultured as monolayer (MON) and sphere (SPH). Fatty acid oxidation activity was measured with a colorimetric kit. FAO was normalized on protein content measured by BCA assay. Data are mean ± SEM (n=3, **p≤0.01, *** p≤0.001; Mann-Whitney U test).

Suppl.Fig.11

A

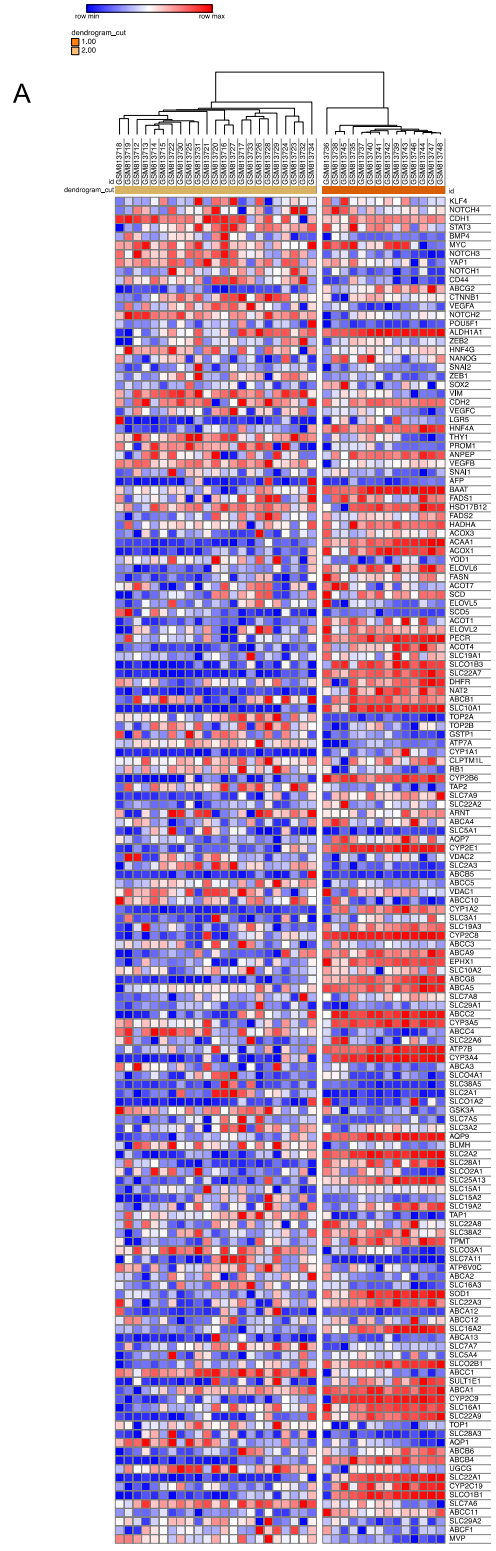

B

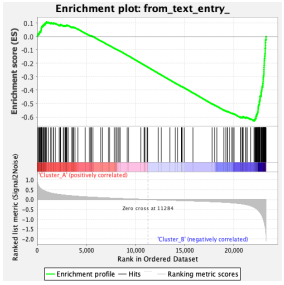

Normalized Enrichment Score (NES)=-1.67
Nominal p-value=0.002

C

FAO

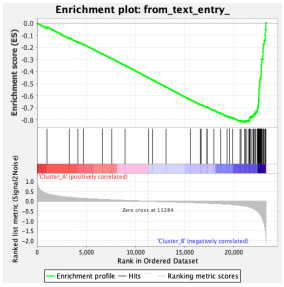

Normalized Enrichment Score (NES)=-1.64
Nominal p-value=0.002

DNL

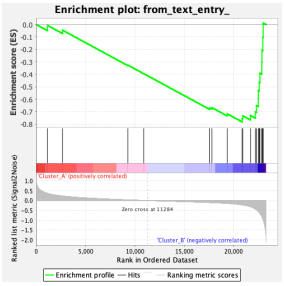

Normalized Enrichment Score (NES)=-1.48
Nominal p-value=0.021

Fig. S11. Classification of CCA patients in terms of stemness and the FA metabolic pathway activity by using public GSE32879 dataset. A) Based on the expression of 139 resistance and stemness genes, hierarchical clustering stratified patients into 2 clusters:
Cluster A: 20 samples, Cluster B: 17 samples. B) Cluster B shows significant enrichment of stemness and resistance genes that was validated with GSEA. C) Next, GSEA was used to associate clusters with curated *de novo* lipogenesis (DNL) and fatty acid beta-oxidation (FAO) gene sets. Both DNL and FAO signatures were significantly enriched in Cluster B. Normalized enrichment score (NES) and p value are reported

Suppl.Fig.12

A

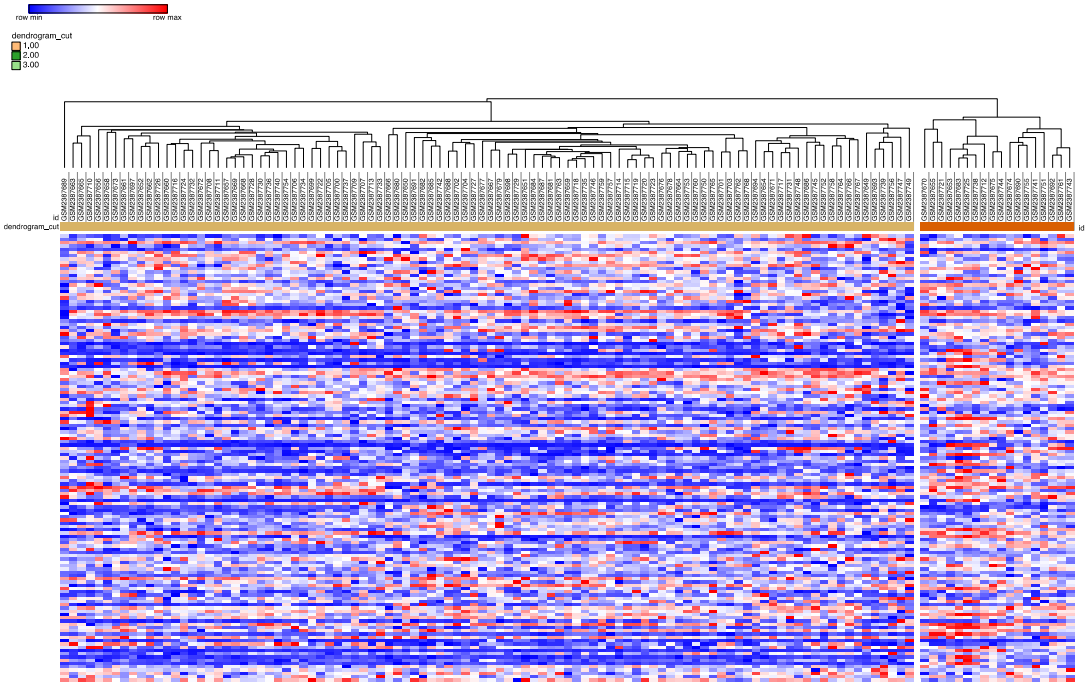

B

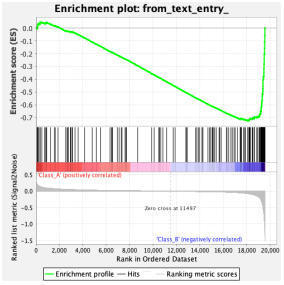

Normalized Enrichment Score (NES)=-1.82
Nominal p-value<0.0001

C

FAO

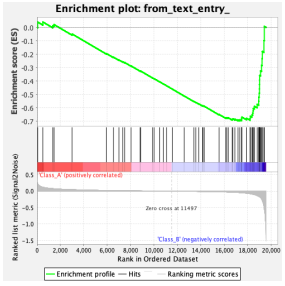

Normalized Enrichment Score (NES)=-1.78
Nominal p-value=0.002

DNL

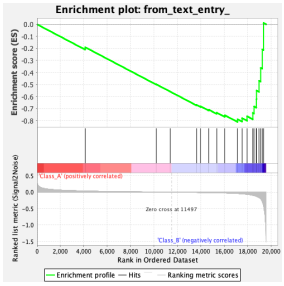

Normalized Enrichment Score (NES)=-1.72
Nominal p-value<0.0001

Fig. S12. Classification of CCA patients in terms of stemness and the FA metabolic pathway activity by using public GSE89749 dataset. A) Based on the expression of 139 resistance and stemness genes, hierarchical clustering stratified patients into 2 clusters: Cluster A: 100 samples, Cluster B: 18 samples. Cluster B shows significant enrichment of stemness and resistance genes that was validated with GSEA. C) Next, GSEA was used to associate clusters with curated *de novo* lipogenesis (DNL) and fatty acid beta-oxidation (FAO) gene sets. Both DNL and FAO signatures were significantly enriched in Cluster B. Normalized enrichment score (NES) and p value are reported

Suppl.Fig.13

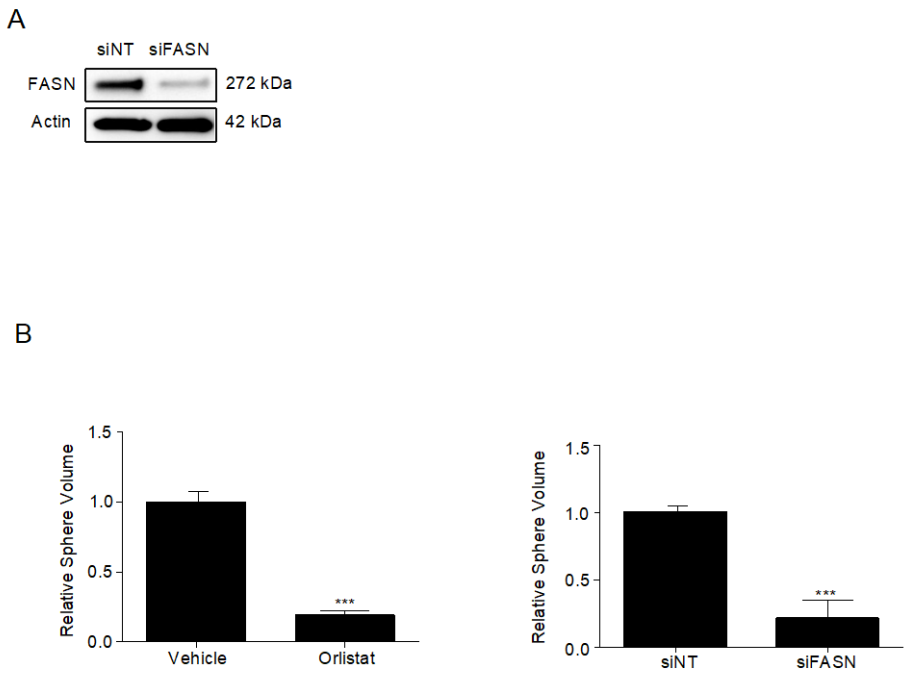

Fig. S13. FASN inhibition affects iCCA SPH forming efficiency. (A) Immunoblot of FASN in CCLP1 SPH transiently silenced for 48 hours. β-Actin immunoblot was performed to ensure equal loading. (B) CCLP1 cells were grown as spheroids for seven days, then treated with orlistat 10μM for 48h. The effect of FASN inhibition on SPH forming efficiency is reported as SPH volume. Data are mean ± SEM (n=3, *** p≤0.001; Mann-Whitney U test). (C) CCLP1 SPH were transiently silenced for 48hours, then cells were counted and sphere forming ability was measured.

Suppl.Fig.14

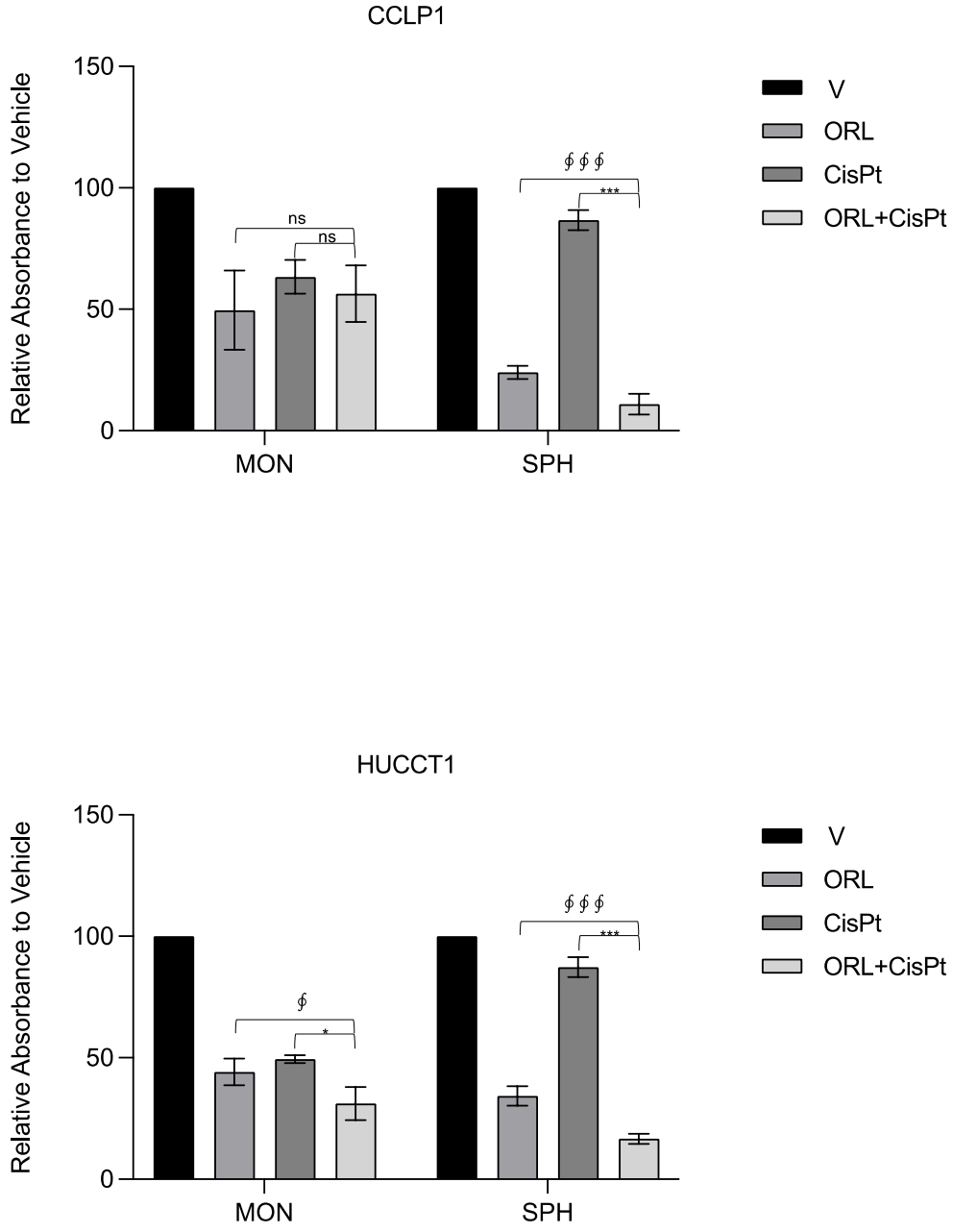

Fig. S14. Orlistat effect on chemoresistance of sphere and monolayer growth. Monolayer (MON) and dissociated sphere (SPH) cells were treated with orlistat (10μM) alone, cisplatin (6μM CCLP1; 15μM HUCCT1) alone and in combination. Cell viability was assessed with crystal violet staining. Data are mean ± SEM (n=3, *p≤0.5, ***p≤0.001, ϕ p≤0.5, ϕϕϕ p≤0.001; Mann-Whitney U test). The * are calculated respect to cisplatin (CisPt), ϕ are calculated respect to orlistat (ORL).

Suppl.Fig.15

A

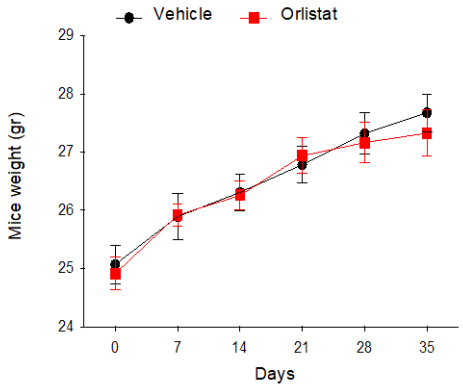

B

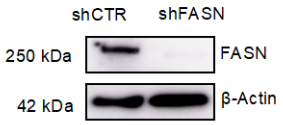

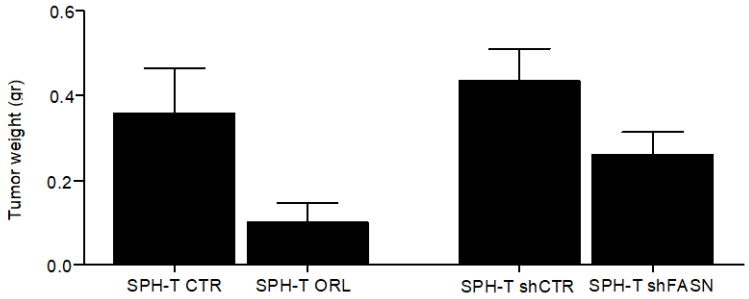

C

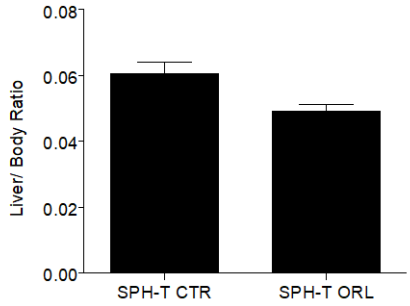

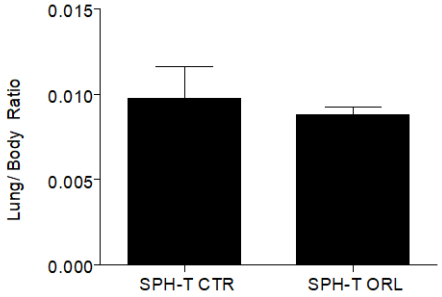

D

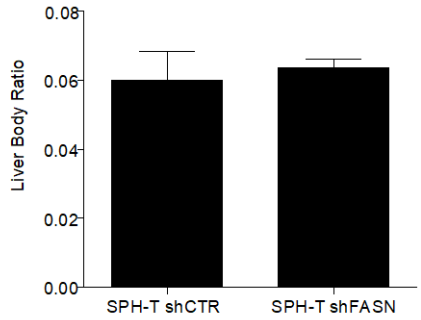

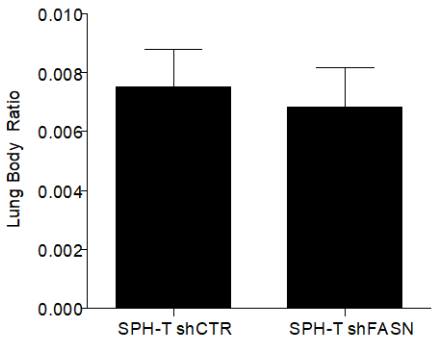

Fig. S15. *In vivo* effects of FASN inhibition. (A) body weight curve for both control and orlistat treated mice without tumor injection. (B) Immunoblot of FASN in CCLP1 SPH stable silenced with shRNA. β-Actin immunoblot was performed to ensure equal loading. Tumors, livers and lungs were collected and weighted at the end of the experiment. C) Weight of generated tumors at 5 weeks after subcutaneous injection into NOD-SCID mice of CCLP1 SPH (***p≤0.001; Mann-Whitney U test). (D,E) Evaluation of orlistat (SPH-T ORL, SPH-T CTR) and shFASN (SPH-T shFASN, SPH-T shCTR) side effects reported as liver body ratio and lung body ratio.

Supplementary tables

Table S1. Effects of fatty acids on iCCA cells proliferation

CCLP1

Oleic acid	24h	48h	72h
66µM	p<0,05	p<0,01	p<0,05
132µM	p<0,01	p<0,001	p<0,001
264µM	p<0,01	p<0,001	p<0,001
528µM	p<0,001	p<0,001	p<0,001

Palmitoleic acid	24h	48h	72h
25µM	ns	ns	ns
50µM	p<0,05	p<0,01	p<0,01
100µM	p<0,01	p<0,001	p<0,01
200µM	p<0,01	p<0,001	p<0,01

HUCCT1

Oleic acid	24h	48h	72h
66µM	ns	ns	ns
132µM	ns	ns	ns
264µM	ns	p<0,01	p<0,01
528µM	p<0,05	p<0,01	p<0,01

Palmitoleic acid	24h	48h	72h
25µM	ns	ns	ns
50µM	ns	p<0,01	p<0,05
100µM	ns	p<0,001	p<0,001
200µM	p<0,01	p<0,001	p<0,01

SG231

Oleic acid	24h	48h	72h
66µM	ns	p<0,05	p<0,05
132µM	p<0,01	p<0,01	p<0,001
264µM	p<0,001	p<0,001	p<0,001
528µM	p<0,001	p<0,001	p<0,001

Palmitoleic acid	24h	48h	72h
25µM	ns	ns	ns
50µM	ns	p<0,05	p<0,01
100µM	p<0,05	p<0,01	p<0,001
200µM	p<0,01	p<0,001	p<0,001

iCCA4

Oleic acid	24h	48h	72h
66µM	ns	p<0,05	p<0,05
132µM	ns	p<0,01	p<0,001
264µM	p<0,01	p<0,001	p<0,001
528µM	p<0,01	p<0,001	p<0,001

Palmitoleic acid	24h	48h	72h
25µM	ns	p<0,05	p<0,05
50µM	p<0,01	p<0,001	p<0,001
100µM	p<0,01	p<0,001	p<0,001
200µM	p<0,01	p<0,001	p<0,001

The table shows p values calculated on oleic or palmitoleic acid treatment for 24h, 48h and 72h in CCLP1, HUCCT1, SG231 and iCCA4 cells. Fatty acids concentrations are reported in the table. (*p≤0,05, ** p≤0,01, *** p≤0,001; Mann-Whitney U test)

Table S2. Effects of fatty acids on iCCA cells proliferation

CCLP1

Linoleic acid	24h	48h	72h
25uM	ns	ns	ns
50uM	ns	ns	ns
100uM	ns	p <0,01	p <0,01
200uM	p <0,05	p <0,001	p <0,001

Palmitic acid	24h	48h	72h
25uM	ns	ns	ns
50uM	ns	ns	ns
100uM	ns	p <0,01	p <0,05
200uM	p <0,01	p <0,001	p <0,001

HUCCT1

Linoleic acid	24h	48h	72h
25uM	ns	ns	ns
50uM	ns	ns	ns
100uM	ns	ns	p <0,01
200uM	ns	p <0,01	p <0,001

Palmitic acid	24h	48h	72h
25uM	ns	ns	ns
50uM	ns	ns	ns
100uM	ns	p <0,05	ns
200uM	p <0,05	p <0,01	p <0,01

The table shows p values calculated on linoleic or palmitic acid treatment for 24h, 48h and 72h in CCLP1, HUCCT cells. Fatty acids concentrations are reported in the table. (*p≤0,05, ** p≤0,01, *** p≤0,001; Mann-Whitney U test)

Table S3. Monounsaturated FAs pretreatment protects iCCA cells from antiblastic toxic effects

CCLP1

	Vehicle	CisPt	OA	POA	CisPt+OA	CisPt+POA
late	0,5%	36,9% ***	0%	1,5%	3,8% ϕϕ	1,8% ϕϕϕ
early	0,3%	8,9% ***	3%	1,5%	3,3% ϕ	3,2%

	Vehicle	OxPt	OA	POA	OxPt+OA	OxPt+POA
late	0,5%	43,7% ***	0%	1,5%	3,2% ϕϕ	1,7% ϕϕϕ
early	0,3%	7,6% ***	3%	1,5%	4,7%	1,3% ϕ

HUCCT1

	Vehicle	CisPt	OA	POA	CisPt+OA	CisPt+POA
late	3%	49,3% ***	3,2%	2,3%	9,4% ϕ	3,2% ϕϕ
early	3,7%	27,4% ***	7%	2,6%	17,2%	3,6% ϕϕ

	Vehicle	OxPt	OA	POA	OxPt+OA	OxPt+POA
late	3%	36% ***	3,2%	2,3%	8,8% ϕ	4,8% ϕϕ
early	3,7%	35% ***	7%	2,6%	9% ϕ	2,6% ϕ

The percentage of early or late apoptotic cells in CCLP1 and HUCCT1 cells treated as reported. **p≤0.01, ***p≤0.001, ϕϕ p≤0.01, ϕϕϕ p≤0.001; Mann-Whitney U test). The * are calculated respect to cisplatin or oxalilplatin, ϕ are calculated respect to vehicle.

Table S4. Enrichr analysis

KEGG 2021 Human

Index	Name	P-value	Adjusted p-value	Odds Ratio	Combined score
1	PI3K-Akt signaling pathway	0.00003672	0.008739	3.37	34.38
2	Small cell lung cancer	0.00008568	0.01020	6.25	58.49
3	Cellular senescence	0.0001528	0.01040	4.51	39.61
4	Kaposi sarcoma-associated herpesvirus infection	0.0002039	0.01040	3.98	33.85
5	Hippo signaling pathway	0.0002186	0.01040	4.30	36.24
6	Epstein-Barr virus infection	0.0003022	0.01143	3.79	30.75
7	Toxoplasmosis	0.0003361	0.01143	5.04	40.31
8	Hypertrophic cardiomyopathy	0.0004719	0.01404	5.51	42.22
9	TGF-beta signaling pathway	0.0006137	0.01623	5.26	38.89
10	Human cytomegalovirus infection	0.0007471	0.01778	3.38	24.35
11	Hepatitis B	0.0009161	0.01881	3.86	26.98
12	Amoebiasis	0.0009980	0.01881	4.81	33.26
13	Chronic myeloid leukemia	0.001106	0.01881	5.59	38.04
14	Pancreatic cancer	0.001106	0.01881	5.59	38.04
15	Pathways in cancer	0.001514	0.02403	2.33	15.12
16	Human immunodeficiency virus 1 infection	0.001680	0.02498	3.25	20.76
17	MAPK signaling pathway	0.002060	0.02861	2.80	17.32
18	Gastric cancer	0.002164	0.02861	3.71	22.76
19	Osteoclast differentiation	0.003495	0.04378	3.81	21.53
20	FoxO signaling pathway	0.004146	0.04531	3.68	20.20
21	Renal cell carcinoma	0.004159	0.04531	5.08	27.84
22	AGE-RAGE signaling pathway in diabetic complications	0.004446	0.04531	4.16	22.51
23	Proteoglycans in cancer	0.004531	0.04531	3.00	16.21
24	Melanoma	0.004989	0.04531	4.85	25.71
25	Non-small cell lung cancer	0.004989	0.04531	4.85	25.71
26	p53 signaling pathway	0.005290	0.04531	4.78	25.05
27	Rap1 signaling pathway	0.005293	0.04531	2.93	15.35
28	Human papillomavirus infection	0.005330	0.04531	2.47	12.93
29	Signaling pathways regulating pluripotency of stem cells	0.006653	0.05460	3.36	16.82
30	Human T-cell leukemia virus 1 infection	0.006910	0.05482	2.80	13.94
31	TNF signaling pathway	0.007667	0.05886	3.68	17.94

MSigDB Hallmark 2020

Index	Name	P-value	Adjusted p-value	Odds Ratio	Combined score
1	Epithelial Mesenchymal Transition	2.048e-9	9.216e-8	6.68	133.58
2	Estrogen Response Early	5.028e-7	0.00001131	5.42	78.56
3	Estrogen Response Late	0.000002742	0.00004112	5.01	64.18
4	TNF-alpha Signaling via NF-kB	0.00006471	0.0007280	4.22	40.71
5	Androgen Response	0.0008879	0.006983	4.92	34.55
6	Cholesterol Homeostasis	0.0009616	0.006983	5.75	39.96
7	p53 Pathway	0.001086	0.006983	3.46	23.59
8	UV Response Dn	0.001746	0.009824	3.85	24.43
9	IL-2/STAT5 Signaling	0.003733	0.01736	3.10	17.33
10	Hypoxia	0.003858	0.01736	3.08	17.14
11	TGF-beta Signaling	0.009429	0.03468	5.19	24.19
12	Mitotic Spindle	0.01199	0.03468	2.73	12.08
13	Apoptosis	0.01232	0.03468	2.96	13.02
14	Myogenesis	0.01233	0.03468	2.72	11.95
15	Interferon Gamma Response	0.01233	0.03468	2.72	11.95
16	Xenobiotic Metabolism	0.01233	0.03468	2.72	11.95

TF Perturbations Followed by Expression

Index	Name	P-value	Adjusted p-value	Odds Ratio	Combined score
1	NFKB1 ACTIVATION HUMAN GSE20736 CREEDSID GENE 2522 UP	1.746e-17	3.369e-14	8.85	341.61
2	EPAS1 KD HUVEC HUMAN GSE62974 RNASEQ UP	1.405e-12	1.356e-9	6.21	169.54
3	GTF2I KO MOUSE GSE48790 CREEDSID GENE 1451 DOWN	1.464e-11	9.420e-9	6.68	166.57
4	EGR3 KD HUMAN GSE52108 CREEDSID GENE 2233 DOWN	2.775e-11	1.339e-8	5.02	121.99
5	GTF2I KO MOUSE GSE48790 CREEDSID GENE 1452 DOWN	4.273e-11	1.649e-8	6.30	150.38
6	POU5F1 KD HUMAN GSE21135 CREEDSID GENE 1328 UP	1.359e-10	4.171e-8	4.99	113.47
7	ARID3A OE MOUSE GSE56853 CREEDSID GENE 1338 UP	1.623e-10	4.171e-8	5.35	120.60
8	FLI1 KD HUMAN GSE27524 CREEDSID GENE 1598 UP	1.729e-10	4.171e-8	4.77	107.17

Index	Name	P-value	Adjusted p-value	Odds Ratio	Combined score
9	SPDEF KD HUMAN GSE40985 CREEDSID GENE 2606 UP	2.069e-10	4.436e-8	5.28	117.81
10	GATA3 OE HUMAN GSE24249 CREEDSID GENE 649 UP	2.788e-10	4.892e-8	5.20	114.44
11	POU5F1 KD MOUSE GSE56853 CREEDSID GENE 1336 UP	2.788e-10	4.892e-8	5.20	114.44
12	ZNF207 OE HUMAN GSE9951 CREEDSID GENE 1581 DOWN	3.737e-10	6.011e-8	5.12	111.20
13	FLI1 KD HUMAN GSE27524 CREEDSID GENE 1599 UP	6.128e-10	8.045e-8	5.20	110.31
14	FLI1 KD HUMAN GSE27524 CREEDSID GENE 1604 UP	6.128e-10	8.045e-8	5.20	110.31
15	WT1 KO MOUSE GSE15325 CREEDSID GENE 2156 UP	6.253e-10	8.045e-8	4.99	105.68
16	DUX4 OE HUMAN GSE33799 CREEDSID GENE 1430 UP	1.098e-9	1.324e-7	5.51	113.71
17	ZNF589 SIRNA MDAMB231 HUMAN GSE79586 RNASEQ DOWN	2.240e-9	2.543e-7	5.55	110.60
18	ATF3 SIRNA HDF HUMAN GSE81405 RNASEQ DOWN	2.947e-9	3.160e-7	5.20	102.16
19	ARID3A OE MOUSE GSE56853 CREEDSID GENE 1339 UP	5.551e-9	5.639e-7	4.80	91.17
20	POU5F1 KD HUMAN GSE21135 CREEDSID GENE 1329 UP	7.938e-9	7.660e-7	4.35	81.20
21	STAT3 SIRNA MDAMB468 HUMAN GSE85579 RNASEQ UP	8.502e-9	7.814e-7	4.68	86.96
22	EZH2 SHRNA HUVEC HUMAN GSE71164 RNASEQ UP	9.859e-9	8.649e-7	5.63	103.83
23	IRX6 SIRNA MDAMB231 HUMAN GSE79586 RNASEQ DOWN	1.039e-8	8.722e-7	5.31	97.65
24	TBX3 SHRNA HFF HUMAN GSE76572 RNASEQ UP	1.161e-8	9.337e-7	4.60	83.98
25	ZEB1 OE CFPAC1 HUMAN GSE64558 RNASEQ DOWN	1.281e-8	9.887e-7	5.53	100.57
26	ETS1 SHRNA DU145 HUMAN GSE59020 RNASEQ UP	2.900e-8	0.000002152	4.20	72.85
27	FLI1 KD HUMAN GSE27524 CREEDSID GENE 1600 UP	3.444e-8	0.000002405	4.31	74.11
28	FLI1 KD HUMAN GSE27524 CREEDSID GENE 1607 UP	3.489e-8	0.000002405	4.68	80.41
29	PAX7 OE H9 HUMAN GSE98976 PROLIFMYOG RNASEQ UP	5.249e-8	0.000003493	4.21	70.51
30	PRRX1 SIRNA BT549 HUMAN GSE79586 RNASEQ DOWN	5.877e-8	0.000003750	4.99	83.07
31	FLI1 KD HUMAN GSE27524 CREEDSID GENE 1601 UP	6.023e-8	0.000003750	4.17	69.36

Index	Name	P-value	Adjusted p-value	Odds Ratio	Combined score
32	PHF20 SHRNA H1792 HUMAN GSE82115 RNASEQ UP	1.035e-7	0.000006239	8.30	133.56
33	ESR1 KD HUMAN GSE37820 CREEDSID GENE 2326 DOWN	1.565e-7	0.000009155	4.44	69.65
34	FLI1 KD HUMAN GSE27524 CREEDSID GENE 1597 UP	1.879e-7	0.00001052	4.20	65.12
35	NEUROG1 OE HUMAN GSE18296 CREEDSID GENE 1426 DOWN	1.907e-7	0.00001052	4.39	67.86
36	NR2F2 KD HUMAN GSE33182 CREEDSID GENE 822 UP	2.016e-7	0.00001081	4.82	74.38
37	MYC OE U2OS HUMAN GSE59819 RNASEQ UP	2.633e-7	0.00001337	5.33	80.78
38	MYC OE U2OS HUMAN GSE66789 RNASEQ UP	2.633e-7	0.00001337	5.33	80.78
39	HSF1 KD HUMAN GSE3697 CREEDSID GENE 782 UP	2.802e-7	0.00001387	5.31	80.04
40	PRRX1 SIRNA MDAMB231 HUMAN GSE79586 RNASEQ DOWN	3.144e-7	0.00001517	4.94	73.95
41	MYB KD HUMAN GSE49286 CREEDSID GENE 1842 DOWN	5.041e-7	0.00002373	4.29	62.26
42	HOXA11 SIRNA MDAMB231 HUMAN GSE79586 RNASEQ DOWN	5.710e-7	0.00002624	5.36	77.03
43	EGR3 KD HUMAN GSE52108 CREEDSID GENE 2231 DOWN	5.857e-7	0.00002629	4.06	58.32
44	ATF3 SIRNA HDF HUMAN GSE81405 RNASEQ UP	6.095e-7	0.00002674	4.45	63.64
45	SPDEF KD HUMAN GSE40985 CREEDSID GENE 2606 DOWN	7.263e-7	0.00003075	4.91	69.43
46	BNC2 SIRNA BT549 HUMAN GSE79586 RNASEQ DOWN	7.330e-7	0.00003075	5.25	74.09
47	GATA3 OE MDAMB231 HUMAN GSE72141 RNASEQ UP	7.557e-7	0.00003103	4.62	65.05
48	HIF1A OE 786O HUMAN GSE67237 RNASEQ UP	9.470e-7	0.00003808	3.93	54.53
49	PIN1 DEPLETION HUMAN GSE26262 CREEDSID GENE 477 UP	9.801e-7	0.00003857	4.52	62.57
50	ZFX KO MOUSE GSE7069 CREEDSID GENE 177 UP	0.000001012	0.00003857	4.08	56.39

Table S5. Clinical pathological data of iCCA patients (n=68)

	Mean	SD
Age	62,63	11,51
Tumor size	64,35	35,78
SEX		
F	29	
M	25	
Unknown	14	
Stage		
2	3	
3	8	
4a	12	
4b	22	
Background disease		
cirrhosis	2	
fibrisis w/o cirrhosis	1	
auto-immune hepatitis/Primary sclerosing cholangitis	1	
Perineural invasion		
Yes	17	
No	29	
ND	22	
Infiltration - potral tract		
Yes	11	
No	25	
ND	32	
Metastatic sites		
lymph nodes	10	
colon	3	
lung	3	
other	6	

Table S6. List of primers

Gene	Sequence
AFP-FW	AAGGCCAGGAACAGGAAGTC
AFP-REV	CACACCGAATGAAAGACTCG
EpCAM-FW	TGTGGTGATAGCAGTTGTTGC
EpCAM-REV	CTATGCATCTCACCCATCTCC
LGR5-FW	CTTCCAACCTCAGCGTCTTC
LGR5-REV	TTTCCCGCAAGACGTAACTC
CD13-FW	CAGTGACACGACGA TTCTCC
CD13-REV	CCTGTTTCCTCGTTGTCCTT
CD133-FW	GCTTCAGGAGTTTCA TGTTGG
CD133-REV	GGGGAATGCCTACATCTGG
NANOG-FW	GTCTCGTATTTGCTGCATCG
NANOG-REV	GAAACACTCGGTGAAATCAGG
BMI1-FW	TTGCTTTGGTCGAACTTGG
BMI1-REV	GTGCTTCTTTTGCAGACTGG
CMYC-FW	CGGAACTCTTGTGCGTAAGG
CMYC-REV	ACTCAGCCAAGGTTGTGAGG
KLF4-FW	AGACAGTCTGTTATGCACTGTGG
KLF4-REV	TGTTCTGCTTAAGGCATACTTGG
SOX-2-FW	ATGGGTTCGGTGGTCAAGT
SOX-2-REV	GGAGGAAGAGGTAACCACAGG
BMP4-FW	AGCGTAGCCCTAAGCATCAC
BMP4-REV	AGTCATTCCAGCCCACATCG
YAP-FW	ACCCTCGTTTTGCCATGAAC
YAP-REV	TTGTTTCAACCGCAGTCTCTC
STAT3-FW	GGCATTCGGGAAGTATTGTCG
STAT3-REV	GGTAGGCGCCTCAGTCGTATC
HNF4-FW	CTCGTCGACATGGACATGGCCGACTAC
HNF4-REV	GGCTTGCTAGATAACTTCCTGCTTGGT
ECAD-FW	AGGCCAAGCAGCAGTACATT
ECAD-REV	A TTCACA TCCAGCACA TCCA
VIM-FW	ACACCCTGCAATCTTTCAGACA
VIM-REV	GATTCCACTTTGCGTTCAAGGT
CTNNB1-FW	GCTGGGACCTTGCATAACCTT
CTNNB1-REV	ATTTTCACCAGGGCAGGAATG
ZEB1-FW	AAGAAAGTGTTACAGATGCAGCTG
ZEB1-REV	CCCTGGTAACACTGTCTGGTC
ZEB2-FW	AGGGACAGA TCAGCACCAAA
ZEB2-REV	GTGCGAACTGTAGGAACCAG
SNAIL-FW	CCTCCCTGTCAGATGAGGAC
SNAIL-REV	CAAGGAATACCTCAGCCTGG
SLUG-FW	ACAGCGAACTGGACACACAT
SLUG-REV	GATGGGGCTGTATGCTCCT
VEGFa-FW	CACTGAGGAGTCCAACATCAC
VEGFa-REV	AGGAAGCTCATCTCTCCTATGT
ABCF1-REV	CCCTTGTATTCATTGATGGC
ABCF1-FW	CTCATCTTGGACGAGCC
ABCC2-REV	GATAGCTGTCCGTACTTTTAC
ABCC2-FW	AAATTGCTGATCTCCTTTGC
ABCB1-REV	AGTCTGCATTCTGGATGG

ABCB1-FW	AGTGAAAAGGTTGTCCAAG
ABCG2-REV	GGCTTTCTACCTGCACGAAAACCAGTTGAG
ABCG2-FW	ATGGCGTTGAGACCAG

Table S7. List of antibodies

Antibody	Manufacturer	Dilution	Catalog number
Phospho AKT (Ser473)	Cell Signaling Technology	1:1000	#9271
AKT	Cell Signaling Technology	1:1000	#9272
Phospho STAT3 (Y705)	Cell Signaling Technology	1:1000	#9145
STAT3	Cell Signaling Technology	1:1000	#30835
Phospho ERK1/2 (Thr2020/Y204)	Cell Signaling Technology	1:1000	#9101
ERK1/2	Cell Signaling Technology	1:1000	#4348
Phospho P38 (Thr180/Y182)	Cell Signaling Technology	1:1000	#4511
P38	Abcam	1:1000	ab59461
cMYC	Cell Signaling Technology	1:1000	#5605
P27	Cell Signaling Technology	1:1000	#3686
P21	Cell Signaling Technology	1:1000	#2947
FASN	Cell Signaling Technology	1:1000	#3180
AceCS1	Cell Signaling Technology	1:1000	#3658
ACSL1	Cell Signaling Technology	1:1000	#9189
ACAC	Cell Signaling Technology	1:1000	#3666
ACLY	Cell Signaling Technology	1:1000	#4332
PPARγ	Cell Signaling Technology	1:1000	#2430
Phospho mTOR (Ser2448)	Cell Signaling Technology	1:1000	#2971
mTOR	Cell Signaling Technology	1:1000	#2983
Phospho S6K (Thr689)	Cell Signaling Technology	1:1000	#9205
S6K	Cell Signaling Technology	1:1000	#9202
β-actin	Sigma Aldrich	1:2500	A5441
Vinculin	Sigma Aldrich	1:2500	V9131

Raw data for western blotting

Fig.3 D

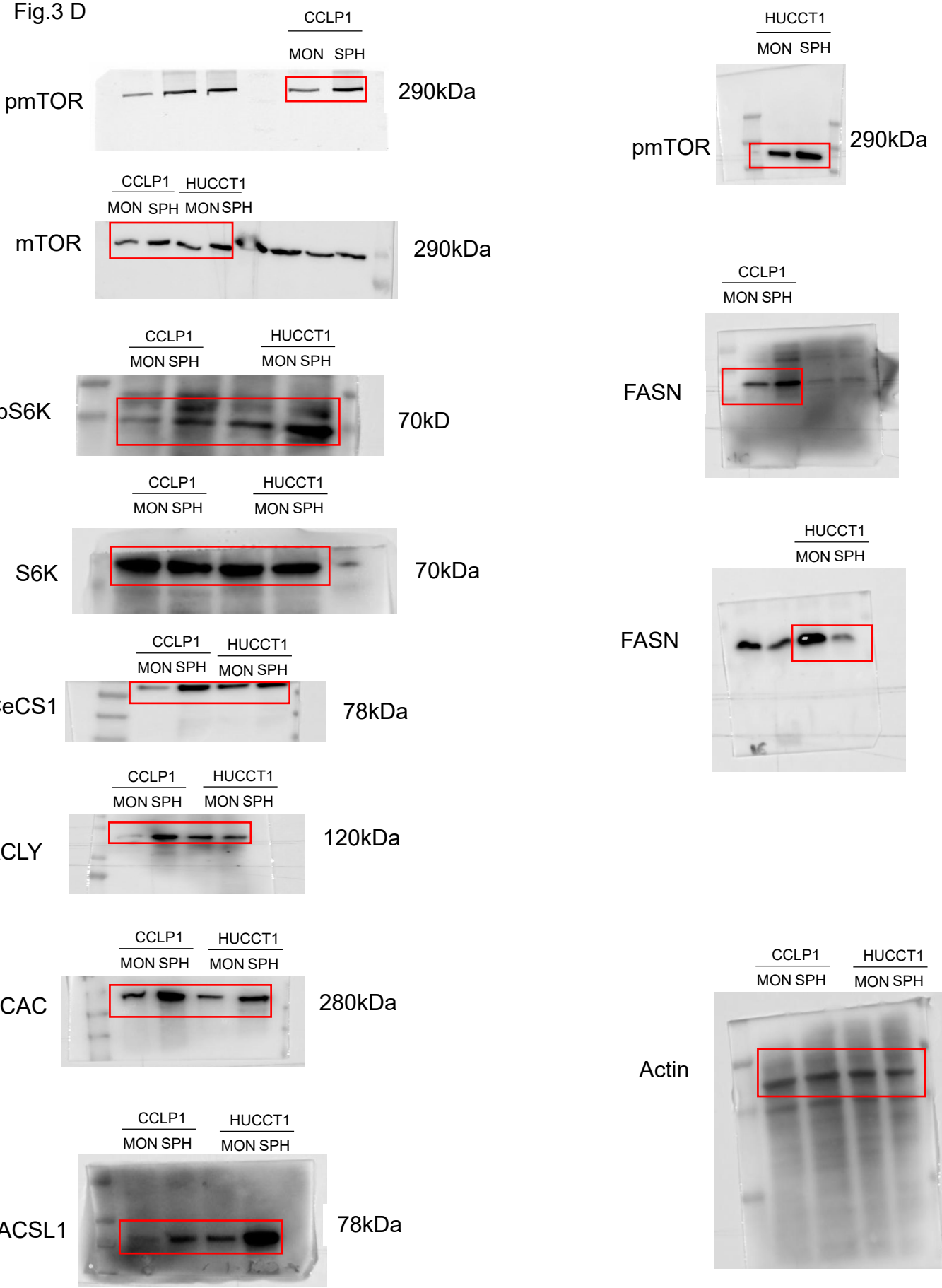

Fig.7 E

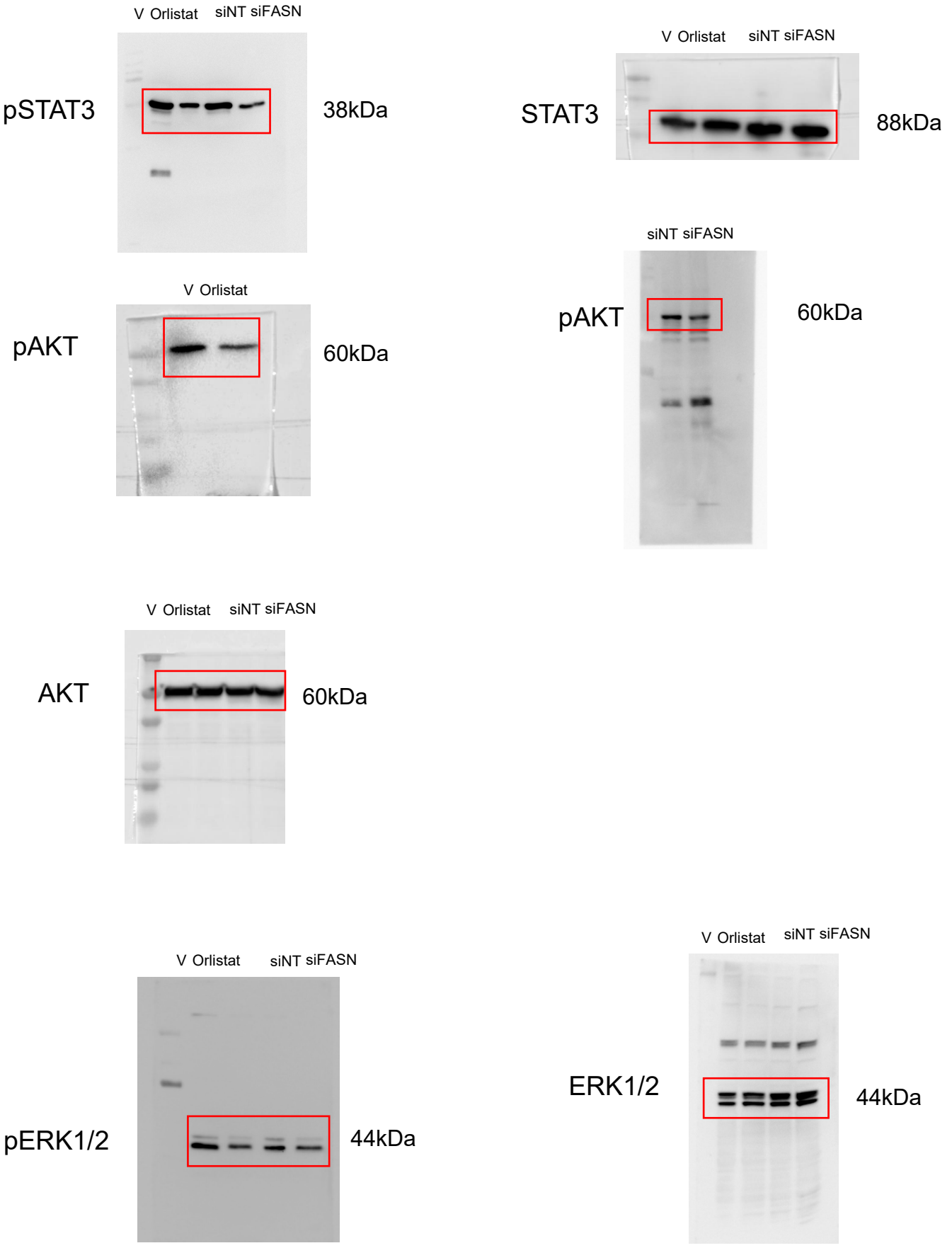
V Orlistat
siNT siFASN
pSTAT3
38kDa
V Orlistat
siNT siFASN
STAT3
88kDa
V Orlistat
pAKT
60kDa
siNT siFASN
pAKT
60kDa
V Orlistat
siNT siFASN
AKT
60kDa
V Orlistat
siNT siFASN
pERK1/2
44kDa
V Orlistat
siNT siFASN
ERK1/2
44kDa

Fig.7 E

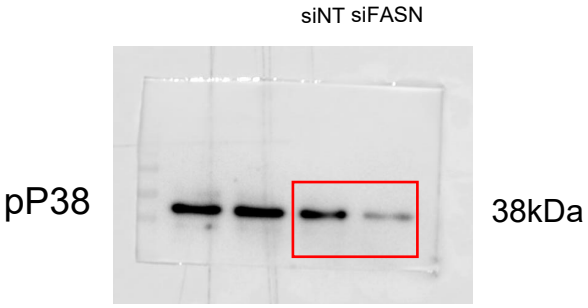
siNT siFASN
pP38
38kDa

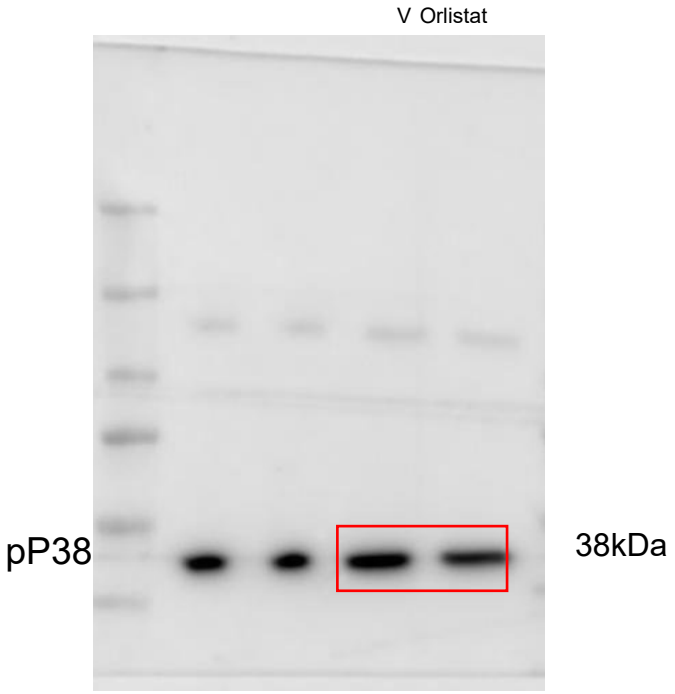
V Orlistat
pP38
38kDa

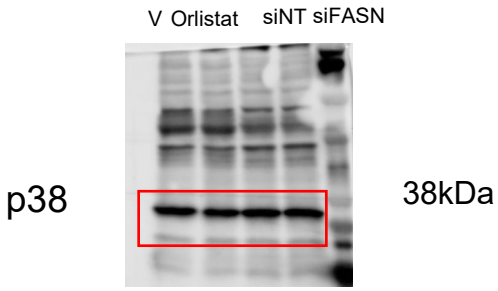
V Orlistat siNT siFASN
p38
38kDa

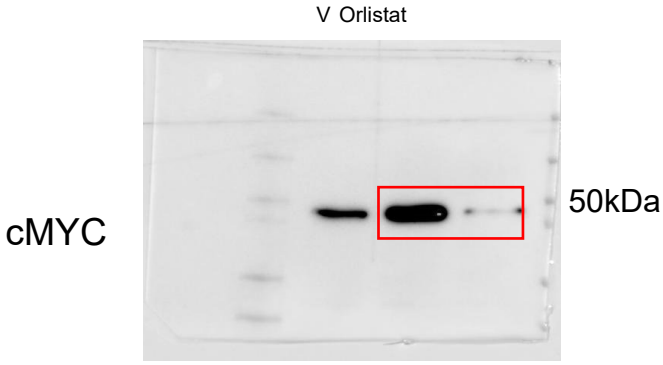
V Orlistat
cMYC
50kDa


siNT siFASN
cMYC
50kDa

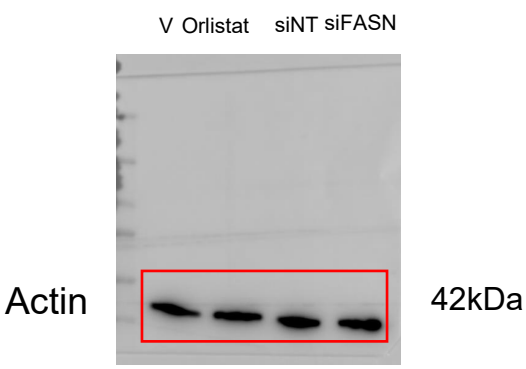
V Orlistat siNT siFASN
Actin
42kDa

Fig.8 F

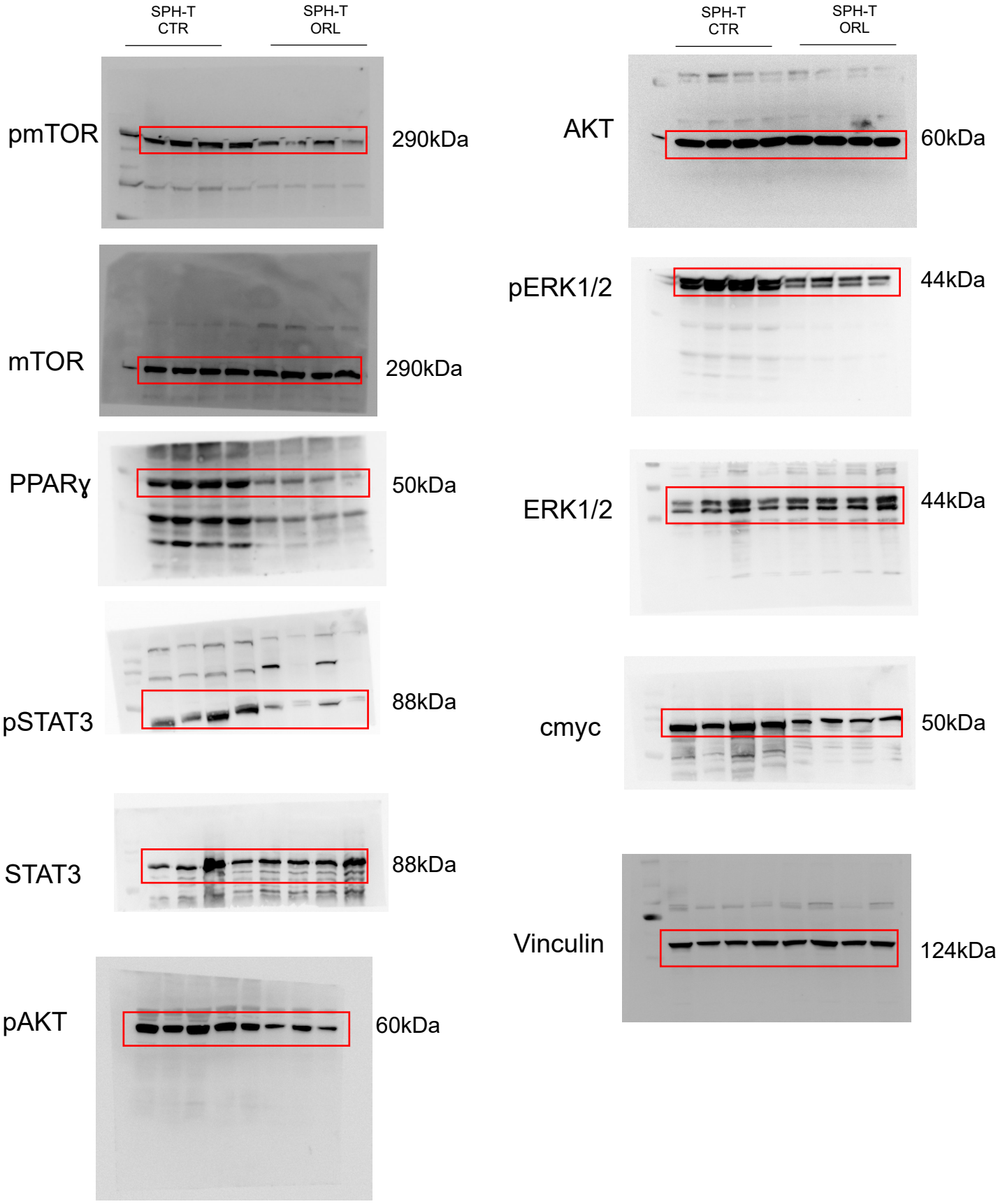
SPH-T CTR
SPH-T ORL
pmTOR
290kDa
mTOR
290kDa
PPARγ
50kDa
pSTAT3
88kDa
STAT3
88kDa
pAKT
60kDa
SPH-T CTR
SPH-T ORL
AKT
60kDa
pERK1/2
44kDa
ERK1/2
44kDa
cmyc
50kDa
Vinculin
124kDa

Fig.8 F

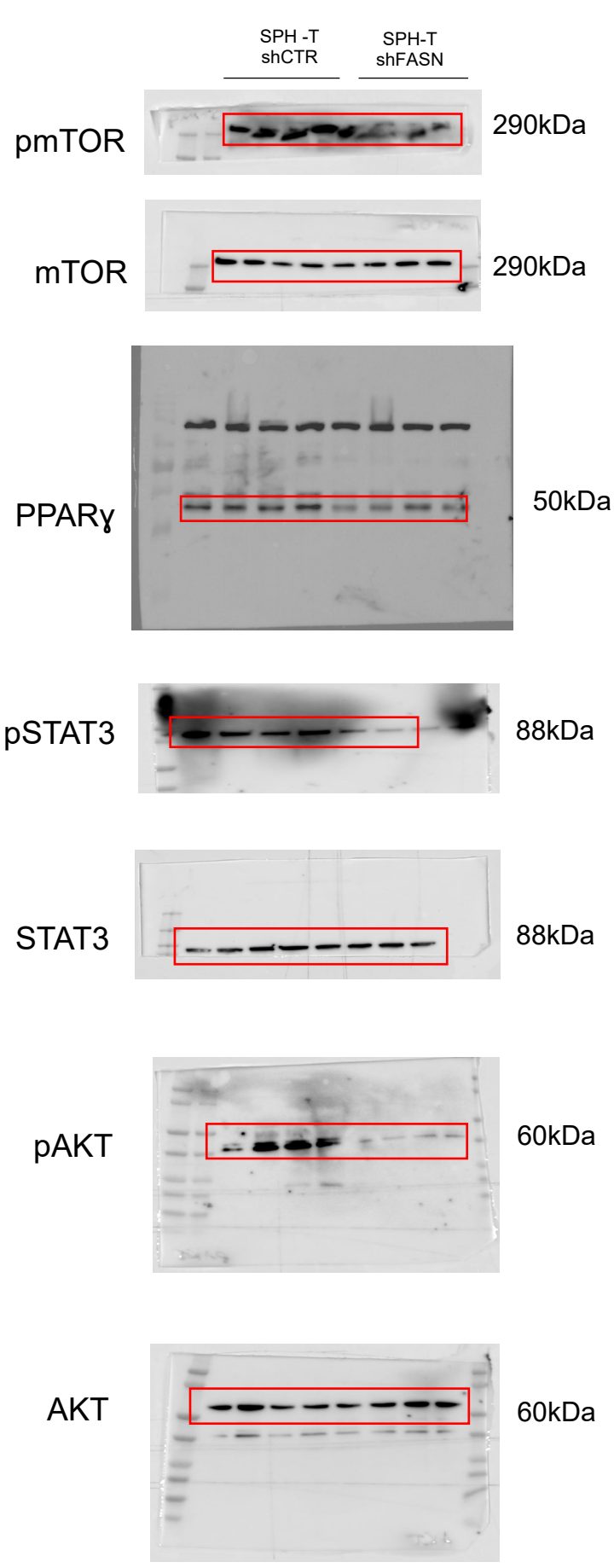
SPH -T shCTR
SPH-T shFASN
pmTOR
290kDa
mTOR
290kDa
PPARγ
50kDa
pSTAT3
88kDa
STAT3
88kDa
pAKT
60kDa
AKT
60kDa

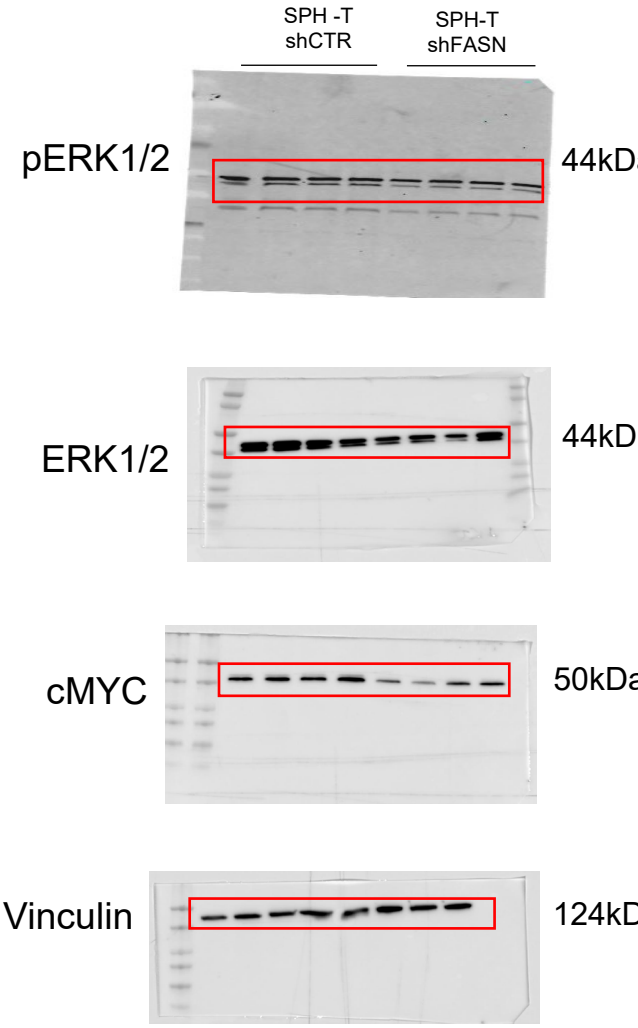
SPH -T shCTR
SPH-T shFASN
pERK1/2
44kD
ERK1/2
44kD
cMYC
50kDa
Vinculin
124kD

Supplementary references
Author names in bold designated shared co-first authorship

1. **Raggi C, Correnti M,** Sica A, et al. Cholangiocarcinoma stem-like subset shapes tumor-initiating niche by educating associated macrophages. J Hepatol 2017;66:102-115.
2. Raggi C, Taddei ML, Sacco E, et al. Mitochondrial oxidative metabolism contributes to a cancer stem cell phenotype in cholangiocarcinoma. J Hepatol 2021;74:1373-1385.
3. Masoodi M, Gastaldelli A, Hyotylainen T, et al. Metabolomics and lipidomics in NAFLD: biomarkers and non-invasive diagnostic tests. Nat Rev Gastroenterol Hepatol 2021;18:835-856.
4. Andersen JB, Spee B, Blechacz BR, et al. Genomic and genetic characterization of cholangiocarcinoma identifies therapeutic targets for tyrosine kinase inhibitors. Gastroenterology 2012;142:1021-1031.e1015.
5. Chen S, Zhou Y, Chen Y, et al. fastp: an ultra-fast all-in-one FASTQ preprocessor. Bioinformatics 2018;34:i884-i890.
6. Patro R, Duggal G, Love MI, et al. Salmon provides fast and bias-aware quantification of transcript expression. Nat Methods 2017;14:417-419.
7. Soneson C, Love MI, Robinson MD. Differential analyses for RNA-seq: transcript-level estimates improve gene-level inferences. F1000Res 2015;4:1521.
8. Smedley D, Haider S, Ballester B, at al. BioMart--biological queries made easy. BMC Genomics 2009;10:22.
9. **Subramanian A, Tamayo P**, Mootha VK, et al. Gene set enrichment analysis: a knowledge-based approach for interpreting genome-wide expression profiles. Proc Natl Acad Sci U S A 2005;102:15545-15550.
10. Mootha VK, Lindgren CM, Eriksson KF, et al. PGC-1alpha-responsive genes involved in oxidative phosphorylation are coordinately downregulated in human diabetes. Nat Genet 2003;34:267-273.
11. Liberzon A, Subramanian A, Pinchback R, et al. Molecular signatures database (MSigDB) 3.0. Bioinformatics 2011;27:1739-1740
12. Liberzon A, Birger C, Thorvaldsdóttir H, et al. The Molecular Signatures Database (MSigDB) hallmark gene set collection. Cell Syst 2015;1:417-425.